VoIP Capacity over Multiple IEEE 802.11 WLANs

CHAN, An

A Thesis Submitted in Partial Fulfillment

of the Requirements for the Degree of

Master of Philosophy

in

Information Engineering

© The Chinese University of Hong Kong

September 2007

摘要

IP 網路語音傳輸技術〔VoIP 或網絡電話，下稱 VoIP〕一般只要求較低的數據傳送率〔如 29.2Kbps〕。相對而言，IEEE 802.11 無線區域網絡〔下簡稱無線區域網絡〕卻擁有很高的數據傳送率。例如，802.11b 網絡的數據傳送率就高達 11Mbps。而 802.11g 網絡的數據傳送率更高達 54Mbps。以簡單除法計算，802.11b 和 802.11g 網絡應可分別容納大約二百及九百個 VoIP 用戶。但早前研究顯示，無線區域網絡傳送語音數據的效率卻是非常低。一個 802.11b 網絡只可容納十二個 VoIP 用戶，而一個 802.11g 網絡亦只可容納六十個用戶。此論文進一步指出，在附近有多個無線區域網絡存在的情況下，無線區域網絡對於 VoIP 的容量則會更低。NS2 仿真顯示，在五乘五、二十五個蜂窩結構的無線區域網絡〔下簡稱五乘五網絡〕中，每個 802.11b 網絡只可平均容納 1.63 個用戶，而每個 802.11g 網絡平均也只有 11.70 個用戶。

在這篇論文中，我們提供了一些提高無線區域網絡中 VoIP 容量的技術。基於衝突圖模型，我們提出了一種基於完全圖的呼叫接入機制。仿真表明，此機制可令 802.11b 中五乘五網絡對 VoIP 的容量增加 53.1%。而如果再加上三個正交頻率信道，此機制更可提高無線區域網絡的容量到每個 802.11b 網絡可容納 7.39 個用戶。

除了使用不同頻率的信道，我們也考慮到將時分复用技術運用在 802.11 的介質訪問控制上，從而增加無線區域網絡中 VoIP 的容量。我們提出一種「粗略」時分多址技術。在該機制中，時間被分成多個粗略的時隙。每個用戶被分配到一個粗略時隙中。被分配到同一時隙中的多個用戶會通過運用 802.11 介質訪問控制機制來接入信道。此技術因為將附近無線區域網絡中相互干擾的用戶用不同的時隙分開，從而減輕了「暴露終端」問題，從而增加無線區域網絡對 VoIP

的容量。研究發現，三〔或四〕個粗略時隙再加上三個正交頻率信道，便可將每個 802.11b 網絡中 VoIP 的容量提高到 10 個用戶〔將每個 802.11g 的容量提高到 58 個用戶〕。相比基於完全圖的呼叫接入機制，粗略時分多址技術可在多個無線區域網絡的情況下，再提昇額外 35.3%的 VoIP 容量。

基於頻道〔時間或頻率〕分配對提高無線區域網絡 VoIP 容量的好處，我們亦對一般無線網絡中的頻道分配問題進行了初步理論研究。透過圖的著色問題，我們證明，一維線性網絡的衝突圖是一個完美圖。因此此類衝突圖中需要的最大著色數〔如正交信道數、時隙數〕與最大團數相同。而二維網絡中的有效頻道分配則較爲複雜，仍然是一個開放課題。

Abstract

IEEE 802.11 WLAN has high data rates (e.g., 11Mbps in 802.11b and 54Mbps in 802.11g/a) while voice stream of VoIP has low data rate requirements (e.g., 29.2Kbps). It may seem that WLAN can support a large number of VoIP sessions: around 200 sessions in 11b network and 900 sessions in 11g network. However, prior work showed that WLAN is highly inefficient for transporting voice data. Only 12 VoIP sessions can be supported by 802.11b WLAN and 60 sessions by 802.11g WLAN. This thesis shows that the already-low VoIP capacity over WLAN is eroded further when there are multiple WLANs in the vicinity to each other (i.e., in the multi-cell scenario). For example, NS2 simulations show that in a 5-by-5, 25-cell WLAN, per-AP VoIP capacity of 802.11b is only 1.63 sessions, while that of 802.11g is only 11.70 sessions.

We present solutions to improve the dismal VoIP capacity over multiple WLANs. Based on a conflict graph model, we propose a clique-based call admission control. Our simulations show that the call admission control can increase the VoIP capacity by 52.1% in a 5-by-5, 25-cell 802.11b WLAN (from 1.63 to 2.48 sessions per AP). If all the three orthogonal frequency channels in 802.11b are used, the clique-based call admission control can boost the per-AP capacity to 7.39 VoIP sessions.

In addition to frequency channels, we explore adding the time dimension to the basic 802.11 protocol to increase VoIP capacity. In particular, we explore a "coarse-grained" time-division multiple-access scheme (CTDMA) in which the time domain is divided into coarse timeslots. Each station is then assigned to one coarse timeslot, and the stations in the same coarse timeslot compete for channel access

using the 802.11 contention-based CSMA mechanism. The idea is that the so-called "exposed-node" problem can be reduced by allocating different time slots to stations of adjacent cells that interfere with each other, We find that with three orthogonal frequency channels and 3 (or 4) coarse timeslots, per-AP VoIP capacity can be boosted to 10 sessions in 802.11b (to 58 VoIP sessions in 802.11g). This constitutes an improvement of 35.3% over the clique-based call admission control with three orthogonal frequency channels.

Motivated by the advantages observed in 802.11 networks with timeslot and frequency-channel assignment, this thesis also provides a preliminary study of the channel assignment problem in general wireless networks. The channel assignment problem corresponds to a graph coloring problem in the general setting. We prove that the conflict graph of a one-dimensional linear wireless network is a perfect graph, so that the maximum number of colors (channels, e.g. timeslots, frequency-channels) required is the same as the maximum clique size. Effective channel assignment in two-dimensional wireless networks is a tough problem that remains open.

Acknowledgement

Contents

Table of Figures

Chapter 1
Introduction

1.1 Motivations and Contributions

Wireless Local Area Networks (WLANs) have gained great popularity in recent years. Many WLAN-related products have been being developed. Voice-over-IP over WLAN (or commercially called "Wi-Fi phone") is a fast developing area and has attracted much attention. Much work [1-5] has been devoted to the study of VoIP (Voice-over-IP) capacity of IEEE 802.11 WLAN. The prior work focuses primarily on the "single-cell" environment in which there is only one isolated WLAN with one access point (AP). This thesis, in contrast, examines the VoIP capacity in the "multi-cell" environment with many WLANs being deployed in the same geographical area. This scenario is common in practice.

Prior investigations have shown that even in the single-cell scenario, the VoIP capacity over WLAN is severely limited due to the various inherent header and protocol overheads. Assuming the GSM 6.10 codec, for example, only 12 VoIP sessions can be supported in an 802.11b WLAN and around 60 sessions can be supported in 802.11g [3, 5].

This thesis finds that the VoIP capacity is further eroded in the multi-cell scenario, and substantially so. For example, our NS2 [6] simulations show that the capacity of a 5-by-5, 25-cell WLAN is only 1.63 VoIP sessions per AP in 802.11b, and 11.70 sessions per AP in 802.11g.

The contributions of this thesis are three-fold:

1   We point out the extremely low VoIP capacity over multiple WLANs – This
     dismal performance has important implications that deserve further attention in
     view of the accelerating productization of VoIP-over-WLAN technologies.

2   We set up a conflict graph model for VoIP over multiple WLANs and explores
     several solutions to increase VoIP capacity per AP. Based on the conflict graph
     model and the size of the cliques in the graph, a clique-based call admission
     control algorithm is proposed. In our NS2 simulations, the call admission
     control algorithm can increase the VoIP capacity in 5-by-5, 25-cell 802.11b
     WLAN by around 50% to 2.48 sessions per AP. If three frequency-channels are
     used, the per-AP capacity is further increased to 7.39 sessions. In addition, we
     also investigate a coarse-grained time-division multiple-access scheme
     (CTDMA) which integrates TDMA with the basic Carrier Sensing Multiple
     Access (CSMA) MAC in 802.11. Compared with the call admission control in
     three-frequency-channel WLAN, CTDMA can further increase the per-AP VoIP
     capacity by another 35% (to 10 sessions in 802.11b WLAN and to 58 sessions
     in 802.11g WLAN).

3   We provide a preliminary study of the channel assignment problem in general
     wireless networks. Specifically, we relate the channel assignment problem with
     theoretical graph coloring. We prove that the conflict graph of a
     one-dimensional linear wireless network is a perfect graph, so that the
     maximum number of colors (channels) required is the same as the maximum
     clique size.

Although VoIP over WLAN has various advantages such as low cost, easy setup,

integration of voice and data networks, and seamless mobility when combined with cellular networks, its actual performance in the real-world environment has not been well tested. While the performance can be acceptable if VoIP-over-WLAN remains unpopular and there are only a few users, the wide adoption of VoIP-over-WLAN, if it ever happens, can actually bring about its downfall with its stretched capacity. Boosting VoIP capacity over multiple WLANs is therefore an interesting area that deserves further attention from the research community.

1.2 Related Works

The capacity of wireless networks has been studied for a long time. References [7, 8] give an analytical model of studying the capacity of a general wireless network, while [9] mainly focuses on the performance of particular IEEE 802.11 networks. All the studies point out that the broadcast nature and the CSMA mechanism in 802.11 MAC protocol limit the total capacity of 802.11 networks.

Much work [1-5] has been devoted to the study of VoIP capacity of WLAN. Scenarios studied include a wide range of situations, including varying channel conditions, delay constraints, voice quality requirement, codec of VoIP used, and so on. As shown in [2, 3, 5], the large packet header and the protocol overhead of CSMA mechanism severely limits the capacity of WLAN for carrying VoIP traffic. Specifically, [3] and [5] showed through NS2 simulations that with GSM 6.10 codec, 802.11b WLAN can support 12 VoIP sessions only.

The prior work, however, focuses primarily on the "single-cell" environment in which there is only one isolated WLAN with one AP, or WLANs are far away from each other so that there are no interference between them. My previous work with

3

Liew [10] has been the first attempt to examine the VoIP capacity in multiple WLANs. It means there are more than one WLAN set up in the vicinity of each other. We refer to it as a "multi-cell" scenario. This thesis develops on the results in [10]. We examine more carefully the capacity of VoIP over multiple WLANs. Different from [10], this thesis uses hexagonal-cells to model the WLAN cells and provides new solutions, such as applying time dimension on 802.11 CSMA MAC, to improve the VoIP capacity over multiple WLANs.

1.3 Organization of the Thesis

The remainder of the thesis is organized as follows. First, we give an overview of the background of IEEE 802.11 networks and VoIP codecs in Chapter 2. Chapter 3 then shows how the CSMA protocol affects the performance of VoIP in terms of capacity. We can see the VoIP capacity is severely eroded in the setting of multiple WLANs. A conflict graph model for analyzing the VoIP capacity over multiple WLANs is developed in Chapter 4. Chapter 4 also presents an immediate solution, a clique-based call admission control algorithm, to improve the VoIP capacity over multiple WLANs. Adding time dimension to the carrier sensing mechanism in 802.11 MAC is discussed in Chapter 5. We also discuss possible realizations of TDMA within the IEEE 802.11 MAC in this chapter. Chapter 6 takes on a theoretical approach to discuss the channel assignment problem in some special wireless networks. Chapter 7 concludes the thesis.

Chapter 2

Background

Before going into the detailed discussion of VoIP capacity over *multiple* WLANs, we first briefly introduce the IEEE 802.11 standard and common VoIP codecs. Our study is based on these two technologies. Then we see how "VoIP over WLAN" combines these two technologies. In this chapter, we also discuss the counter-intuitively low VoIP capacity in an isolated WLAN as shown in previous work. An 802.11b WLAN can only support 12 VoIP sessions, while an 802.11g WLAN can only support 60 sessions.

2.1 IEEE 802.11

2.1.1 Basic IEEE 802.11 Standard

IEEE 802.11 standard has two access mechanisms, Distributed Coordination Function (DCF) and Point Coordination Function (PCF) [11]. The optional PCF is a centralized mechanism and there is a central coordinator to poll other stations for contention-free access to the channel. PCF is proposed to provide a certain level of Quality of Service (QoS), but PCF is not supported in most of commercial products.
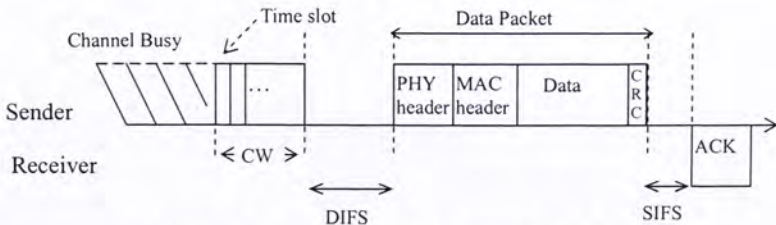
Figure 2-1: Basic Mode of IEEE 802.11 DCF

DCF is the widely used MAC function in practice, and it is based on the Carrier

Sensing Multiple Access with Collision Avoidance (CSMA/CA) protocol. There are

two transmission modes in DCF, Basic Mode and RTS/CST Mode. The transmission

mechanism of Basic Mode is shown in Figure 2-1. Stations continuously sense the

wireless channel. When the channel is sensed idle and a station (sender) has a packet

to send, the sender will randomly choose a backoff time with number of time slots

ranging from 0 to Contention Window (CW) – 1 and start progressively decreasing

the backoff time as long as the channel is idle. When the backoff time reaches zero,

data packet is sent after a DCF Inter Frame Space (DIFS). Once the receiver

receives the packet correctly, it responds with an ACK after a Short Inter Frame

Space (SIFS). In RTS/CTS Mode, instead of sending Data packet after DIFS, the

sender will send a RTS (Ready-to-Send) packet. The receiver will reply a CTS

(Clear-to-Send) packet after a SIFS to sender after receiving the RTS packet. Once

the sender receives the CTS, it sends the data packet after a SIFS. Other stations

(neither the sender nor the receiver) set the NAV (Network Allocation Vector) as

they hear either RTS or CTS packets to reserve the channel for the transmission to

complete. They count down from NAV to zero. When NAV is non-zero, the wireless
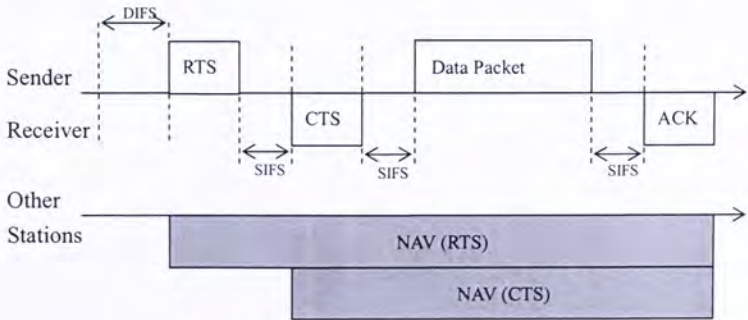
Figure 2-2: RTS/CTS Mode of IEEE 802.11 DCF

medium is indicated busy, so other stations will not try to access the medium. The transmission mechanism of RTS/CTS Mode is shown in Figure 2-2. Although RTS/CTS Mode can partly solve the Hidden Node (HN) problem, it creates large overhead for data transmission, especially when the data packet size is small, such as voice data. Therefore, in VoIP-over-WLAN application, Basic Mode (no RTS/CTS handshake) is commonly used. For details of DCF, readers may refer to [11]. Most work on VoIP over WLAN assumes the use of DCF, and only some consider PCF.

A variety of standards have been defined in the IEEE 802.11 standard family. IEEE 802.11b [12] operates in the 2.4GHz frequency band and it supports data rates up to 11Mbps, while IEEE 802.11g [13] operates in the same frequency band and supports data rates up to 54Mbps. Currently, 802.11b and 802.11g are the most widely deployed standards for WLAN. IEEE 802.11a [14] can also provide data rates up to 54Mbps, but it operates in regulated frequency band (license is needed). So, it is less commonly deployed.

2.1.2 Types of Networks

There are two types of networks supported in IEEE 802.11 WLAN, ad-hoc network
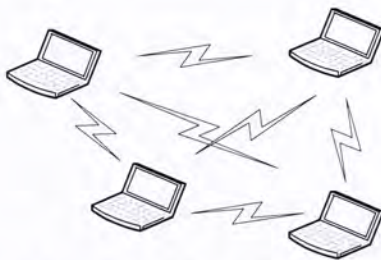
Figure 2-3: An ad-hoc network
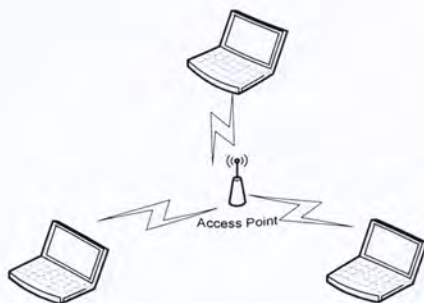
Figure 2-4: An infrastructure network

and infrastructure network. Figures 2-3 and 2-4 show an ad-hoc network and an infrastructure network respectively.

In an ad-hoc network, as shown in Figure 2-3, wireless stations form a local network communicate directly with each other. No centralized coordinator is required in an ad-hoc network. An infrastructure network, on the other hand, has a centralized unit, called access point (AP), to coordinate all the network traffic. As shown in Figure 2-4, wireless stations communicate with each other through AP.

Our study of VoIP over WLAN assumes the infrastructure network. Voice packets are transmitted to and from AP (bidirectional). Although our numerical studies assume the infrastructure-mode WLAN, the techniques and principles demonstrated in this thesis can also be applied to ad hoc networks.

2.2 Voice over IP (VoIP) Codecs

In a VoIP system, voice signals are encoded and compressed into a low-rate packet stream by codecs. Although there are various codecs with different attributes, small

Table 2-1: Attributes of Commonly Used Codecs

Codec	Bit Rate (Kbps)	Framing Interval (ms)	Payload (Bytes)	Packet per second
GSM 6.10	13.2	20	33	50
G. 711	64	20	160	50
G. 723.1*	5.3/6.3	30	20/40	33
G. 729	8	10	10	50**

* G.723.1 has two standards, so some of its attributes have two values.
** In G. 729, two frames are combined into one packet.

voice packet payload (ranging from 10 to 30 bytes) and relatively large IP/UDP/RTP

headers (40-byte) are the common characteristic among them. Table 2-1 shows some

VoIP codecs and their attributes.

2.3 VoIP over WLAN

2.3.1 System Architecture of VoIP over WLAN

The prior work [1-5] focuses primarily on the "single-cell" environment in which

there is only one isolated WLAN with one access point (AP). Figure 2-5 shows the

system architecture they assumed for VoIP-over-WLAN.

As shown in Figure 2-5, each 802.11 WLAN is referred to as a basic service set

(BSS) in the standard specification. As mentioned in Section 2.1.2, infrastructure

network is used. The system architecture assumes that all voice streams transferred

between users via AP, since users seldom call their neighbors within the same BSS.

The system architecture further assumes the WLANs are far away from each other

(i.e. they are isolated), so that there is no interference between them. The part of

wireless communication is the transmission of voice streams between AP and

wireless stations. The research of VoIP capacity over WLAN focuses on this part.
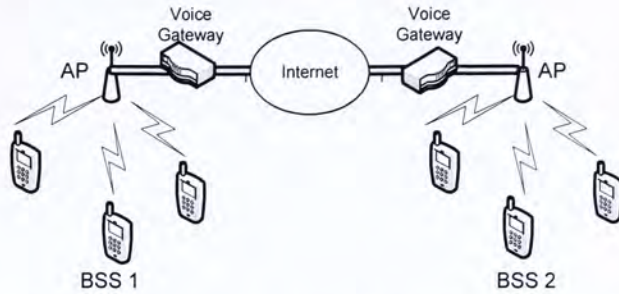
Figure 2-5: System architecture of VoIP over isolated WLANs

This thesis also focuses on the transmission of voice streams between the AP and its wireless stations. In a BSS, there are two kinds of voice streams for each VoIP session. The uplink stream is the voice packets originating from the wireless station to its AP, while the downlink stream is voice packets from AP to its stations. The voice streams between different APs can be delivered by backbone wired network, and it is out of the scope of this thesis. We also assume the similar system architecture shown in Figure 2-5. The only difference is that we assume there are multiple WLANs deployed in the same geographical area. This means WLANs may interfere with each other. We refer to this scenario as "multi-cell" WLAN, and it is common in practice.

2.3.2 VoIP Capacity over an Isolated WLAN

VoIP packets are streams of packets containing encoded voice signals. There are different codecs for encoding voice signals. Take GSM 6.10 as an example. The voice payload is 33-byte and 50 packets are generated in each second. After adding the 40-byte IP/UDP/RTP header, the minimum channel capacity to support a GSM 6.10 voice stream in one direction (either uplink or downlink) is 29.2Kbps.

Intuitively, an 802.11b WLAN can support nearly 200 VoIP sessions (divide 11Mbps

by two times of 29.2Kbps); and for 802.11g, more than 900 sessions (divide 54 Mbps by two times of 29.2Kbps). However, prior investigation has shown that the VoIP capacity is severely limited due to the various inherent header and protocol overheads (e.g. backoff countdown time, Physical Header of 802.11 packet, etc.). With the GSM 6.10 codec, for example, only 12 VoIP sessions can be supported in an 802.11b WLAN; and 60 sessions in 802.11g [3, 5].

Prior work has primarily focused on VoIP over an isolated WLAN. When multiple WLANs are in the proximity of each other, their VoIP sessions may compete with each other for airtime usage if these WLANs use the same frequency channels. In 802.11b/g, for example, there are only three orthogonal channels, but it is common to see many overlapping WLANs in a building these days. We show in this thesis that the already-low efficiency of VoIP over a single WLAN will be further eroded in such a situation, so much so that only an average of less than two VoIP sessions per AP can be supported in a 5x5, 25-cell, 802.11b WLANs; and less than 12 VoIP sessions for 802.11g. In the next Chapter, we examine how multiple WLANs degrade the VoIP capacity.

Chapter 3
VoIP Capacity over Multiple WLANs

In this chapter, we state our multi-cell topology settings and assumptions for the study of VoIP over multiple WLANs. Although some previous work [7-9] give state-of-art analyses on the capacity of wireless network, they are not closely relevant to our study. Refs. [7-8] derived the capacity of "generic network" and it is not specific to VoIP over multiple WLANs, in which QoS requirements, such as packet-loss rate, need to be considered. Ref. [9], on the other hand, derived the capacity of WLAN where number of stations is kept below the capacity. As in [9], the network capacity is not in terms of number of stations but the total throughput. If the number of stations reaches the network capacity, some stations may suffer starvation which will violate QoS required by VoIP. In our study, we try to put as many as possible stations into WLANs (to measure the network capacity), and the network saturation (exceeding the capacity) is prevented by call admission control which will be discussed in the next chapter. From the NS2 simulation results, we observe the extremely low VoIP capacity over multiple WLANs. We also discuss that the traditional careful frequency channel assignment on multi-cell topology cannot solve the problem of the dismal VoIP capacity.

3.1 Topology Settings and Assumptions

For concreteness, our studies assume the use of GSM 6.10. However, the general issues addressed in this paper are the same for other codecs. We also assume the use of 802.11 Distributed Coordination Function (DCF) [11] MAC protocol and Basic Mode. Although Point Coordination Function (PCF) [11] is also worth studying, it is

not popular and almost never deployed in practice. This is perhaps because (i) PCF is not supported in most 802.11 products and that (ii) the robustness of PCF in real field deployment has not been well tested, particularly in situations where there are multiple mutually-interfering APs in the vicinity of each other serving as the point coordinators. For our simulations and analyses, we primarily focus on 802.11b and 802.11g.

For the GSM 6.10 codec, as mentioned in Section 2.3.2, the minimum channel capacity to support a voice stream in one direction (either uplink or downlink) is 29.2Kbps. If we allow a packet-loss rate of 1% to 3%, the minimum channel capacity requirement is 28.32Kbps. We use this minimum channel capacity requirement as a benchmark in the evaluation of the capacity of VoIP over WLAN. If both the uplink and downlink of a VoIP session can have throughputs exceeding this benchmark, we say the VoIP session can be "*supported*" in the WLAN.

To evaluate the VoIP capacity over multiple WLANs, we model a "WLAN cell" with a hexagonal area with side of 250m. An AP is placed at the center of the cell. Any wireless client station inside the cell will be associated with the AP. The longest link distance (d_{max}) is 250m, which is the data transmission range (*TXRange*) for 802.11b assumed in NS2 [6]. By placing the cells side by side, we form a D-by-D multi-cell topology, where D is the number of cells on each side. Figure 3-1 shows a 3-by-3 multi-cell topology.
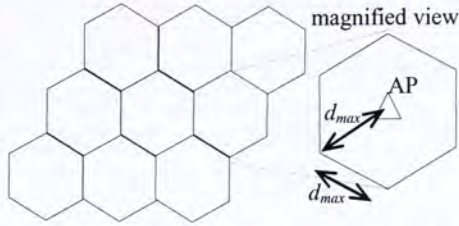
Figure 3-1: A 3-by-3 multi-cell topology

We also assume the carrier sensing range (*CSRange*) of all wireless stations is 550m, which is assumed in NS2 simulator. In real equipments, the operating parameters are always based on "power thresholds" rather than "distances". But for convenience, we will continue to use the "distance" concepts (e.g., *TXRange*, *CSRange*, etc.) to describe the system operation. For actual carrier-sensing operation and for detection, it is the power received that matters rather than the distance. We will see that implementation based strictly on the "geometric" distance interpretation is unnecessary once we move on to the graph-theoretic formulation later in this thesis. Distances only matters to performance rather than to the logical correctness of system operation. "Distance" is interpreted in a virtual sense in the following. Specifically, two wireless stations i and j are said to be separated by a virtual distance $d_{i,j}$ if the power they receive from each other satisfies (1) as follows:

$$P_{i,j} = P_{j,i} = k / d_{i,j}^{\alpha} \tag{1}$$

where k is a constant, α is a "reference" (not the actual) path-loss exponent, assuming all stations use the same transmit power. With the same k and reference α applied to the whole network, we can then derive the virtual distance $d_{i,j}$ from the measured power transferred, $P_{i,j}$. Given a power threshold requirement, there is then a corresponding virtual-distance requirement. When we say the *CSRange* is set

14

to d_{CS}, we mean the carrier-sensing threshold power is set to $P_{CS} = k/d_{CS}^{\alpha}$ where

α is the nominal constant adopted (e.g., $\alpha = 4$). In the following analyses and

NS2 simulations, we assume $\alpha = 4$. In the subsequent discussions, we assume

there is an underlying scheme to find out $P_{i,j}$, hence, $d_{i,j}$, so that interference

relationship between different links can be found. To limit our scope, we will not

discuss the $d_{i,j}$ discovery algorithms here. The reader is referred to [19] for

possible schemes.

In actuality, two virtual distances of different values may correspond to the same

physical distance, and vice versa, because the actual α (not the reference) for

them are different due to the inhomogeneity in the propagation environment.

For NS2 simulations in the next section, we assume a simplistic call admission

scheme is used.

Definition 1: Simplistic Call Admission Scheme

When the next newly added VoIP session causes a violation of the packet-loss rate

requirement (1% to 3%) by at least one of the sessions in the multi-cell WLAN, we

say that the capacity limit has been exceeded. Upon the unacceptable performance

caused by the newly added session, the newly session will be dropped, and no more

future sessions will be accepted.

The reason no more future sessions will be accepted in Simplistic Call Admission

Scheme is simply because the adding and dropping of QoS-violating sessions can be

quite disruptive to the quality of the existing sessions. We will later consider a

15

Table 3-1: VoIP Capacity over *D*-by-*D* Multi-Cell Topologies

D	1	2	3	4	5
Avg. C_{DxD} in 11b	12.0	12.3	20.0	30.0	40.8
Avg. C_{DxD} in 11g	55.0	79.6	131.8	207.6	292.4

cleverer call admission scheme based on a clique analysis of a conflict graph so that we can "predict" the performance before deciding whether to admit a call to get rid of the disruptiveness.

3.2 Low VoIP Capacity Found in NS2 Simulations

We have set a *D*-by-*D* multi-cell topology as described in Section 3.1. We ran NS2 simulation experiments for *D* =1, 2, 3, 4, and 5. In each run, wireless stations (VoIP sessions) are added one by one randomly assuming uniform distribution. When a particular cell has 12 stations in the 802.11b case (60 stations for the 802.11g case), no more stations will be added to that cell to ensure the capacity of single isolated WLAN is not being exceeded. With each additional VoIP session, NS2 simulation is run and the throughput of each link recorded. With the assumption of Simplistic Call Admission Scheme, we measured the number of VoIP sessions the *D*-by-*D* multi-cell WLAN can support on average. Our simulation results are shown in Table 3-1.

In Table 3-1, $C_{D \times D}$ is the total number of VoIP sessions that can be supported in a *D*-by-*D* multi-cell topology. Obviously, as *D* increases, more VoIP sessions can be supported. We further calculate C_{AP_D}, the per-AP capacity in a *D*-by-*D* multi-cell WLAN, defined as follows:

$$C_{AP\_D} = C_{D \times D} / D^2 \qquad (2)$$
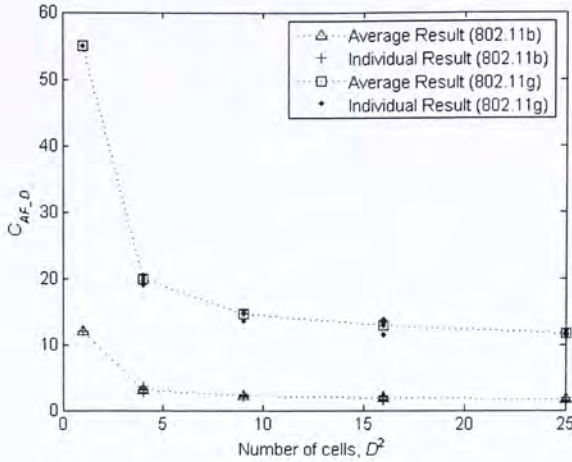
Figure 3-2: Per-AP capacity of D-by-D multi-cell WLAN

We plot C_{AP_D} against number of cells, D^2, in Figure 3-2. We find that as the number

of cells increases, per-AP capacity decreases. When the number of cells is 25, i.e. D

= 5, only 1.63 VoIP sessions can be supported by each AP in 802.11b. Compared

with the single-cell scenario, where each AP can support 12 VoIP sessions in

802.11b, this is a rather large penalty. Similar capacity penalty is also observed in

802.11g WLAN[1].

We also note in passing that for a network larger than the 5-by-5 network, most cells

will be surrounded by six adjacent cells and there will be proportionately fewer cells

at the boundary. One can therefore expect the VoIP capacity per AP to drop even

further when the dimensions are larger than 5-by-5. Actually, in a 10-by-10, 100-cell,

802.11b WLAN, our simulation shows that the per-AP capacity is only 1.22

---

[1]   The VoIP capacity of single-cell 802.11g WLAN measured in simulation is 55.0, not 60
as calculated in [3, 5]. It is due to the smaller minimum contention window size in 802.11g.
But for consistency, we still take "60 VoIP sessions" as the theoretical upper bound for VoIP
capacity over single isolated 802.11g WLAN in our following discussions.

sessions.

3.3 Applying Frequency Channel Assignment

To reduce the mutual interference of neighboring cells, a quick solution is to assign different frequency channels to different cells, as in cellular telephone networks. If there are enough frequency channels, the neighbor cells that could interfere with each other through packet collisions and carrier sensing could be assigned different frequency channels. This boils down to the same situation as in the single-cell case, so that the per-AP VoIP capacity in the multi-cell case is the same as that in the single-cell case. However, we will see in this subsection that careful frequency-channel assignment actually does not help much in improving VoIP capacity over multiple WLANs.

IEEE 802.11b/g has only three orthogonal frequency channels, and this is not enough to completely isolate co-channel interference between cells. Figure 3-3 shows that if we have only three frequency channels, then the nearest distance between two cells using the same channel is the same as the maximum link length within a cell, d_{max}. Since these two cells may interfere with each other, the carrier-sensing range (*CSRange*) should be larger than $3d_{max}$ to avoid hidden-node collisions between the two cells (consider link (AP1, STA1) and link (AP2, STA2) of the two cells, where the distance between STA1 and STA2 is d_{max}; carrier-sensing range of $3d_{max}$ is needed to avoid hidden-node collisions between these two links). Since a cell must now share airtime with other cells, the VoIP capacity per AP cannot be the same as that in the single-cell case. We will discuss more about the impact of three frequency-channel assignment on VoIP capacity over multiple WLANs in the next chapter.
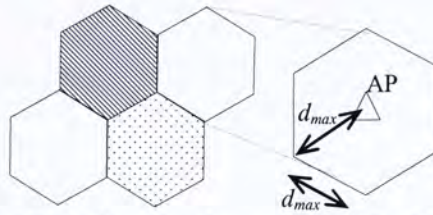
Figure 3-3: 3-channel assignment in multi-cell WLAN
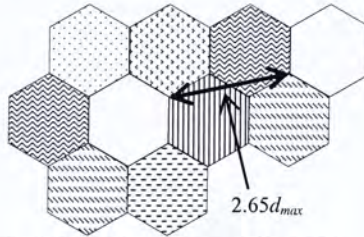
Figure 3-4: 7-channel assignment in multi-cell WLAN

IEEE 802.11a, on the other hand, has 12 orthogonal channels. Figure 3-4 shows that a 7-channel assignment is enough for complete isolation of co-channel interference. The nearest distance between two cells using the same channel is $2.65d_{max}$ which is larger than the minimum *CSRange*, $2d_{max}$, used to prevent collisions within a cell. Thus, with 7-channel assignment, co-channel interference can be completely isolated. However, if we simply use 7 overlay networks in each cell (put 7 APs inside each cell and operate in different channels), the number of VoIP sessions that can be supported in each cell can also be increased by 7 times of that in the single-channel multi-cell topology. Therefore, we find that the channel assignment in Figure 3-4 actually may not improve the VoIP capacity on a per-frequency channel basis, although on a per-AP basis, it does. Furthermore, IEEE 802.11a operates in regulated frequency band (license is needed), so it is not commonly deployed.

19

In the next chapter, we analyze the capacity of VoIP over multiple WLANs and propose a quick solution to the dismally low capacity observed.

Chapter 4

Clique Analysis and Call Admission Control

To understand the cause for the heavy performance penalty of VoIP over multiple WLANs, we consider here a clique analysis based on a graph model that captures the conflict and interference among the nodes. The clique analysis also suggests a call admission methodology. With this call admission scheme, the VoIP capacity can be increased to 2.48 sessions per AP from 1.63 in the 5-by-5, 25-cell 802.11b WLAN. It is a 52.1% improvement.

4.1 Conflict Graph Model and Cliques

Conflict Graph Model

A vertex represents a VoIP session (wireless link).

An edge between two vertices means that the two VoIP sessions compete for the airtime. In other words, they cannot transmit at the same time.

There are two reasons why they cannot transmit at the same time. (i) First, nodes of the two sessions that are within the *CSRange* of each other will be prevented by the IEEE 802.11 protocol from transmitting together. (ii) Even if the two sessions are not within each other's *CSRange*, there may be mutual interference between them so that either one or both of their transmissions will fail if they transmit together: this is due to the well- known hidden-node (HN) problem [15]. In either case (i) or (ii), an edge is drawn between the two vertices of the VoIP sessions to mean that their transmissions cannot use the same airtime. A clique is a subset of vertices in which

there is an edge between any of two vertices [16]. The vertices in a clique compete for the common airtime. That is, the sum of the fractions of airtimes used by the vertices should not exceed one.

In the single-cell scenario, all client stations are within the same cell and associated with the same AP. So, edges should be drawn among all vertices of the same cell. In an 802.11b single-cell WLAN, the maximum clique size is 12, because 12 VoIP sessions will fill up all airtimes. In an 802.11g single-cell WLAN, the maximum clique size is 60.

4.2 Cliques in Multi-Cell WLANs

In a multi-cell WLAN, VoIP sessions of different cells may be outside the *CSRange* and interference range of each other. That means we can find pairs of vertices between which there is no edge, and therefore their transmissions can share the same airtime. Figure 4-1 shows an example of such VoIP sessions. The nearest distance between the four shaded cells is 866m, and therefore the nodes inside different shaded cells cannot sense each other if the *CSRange* is 550m, the default setting in NS2. In other words, case (i) mentioned in Section 4.1 is not satisfied. For case (ii), we consider the *Interference Range (IR)* defined as follows:

$$IR_k = (1+\Delta)d_k \tag{3}$$

where IR_k is the *Interference Range* of a node, k, (it can be either a wireless client station or an AP), d_k is the length of the link associated with the node k; and Δ is a distance margin for interference-free reception with typical value of 0.78 [6, 15]. Within a radius of IR_k, any other transmission will interfere with the node k's reception of the signal. The maximum link length within a cell in Figure 4-1 is d_{max}
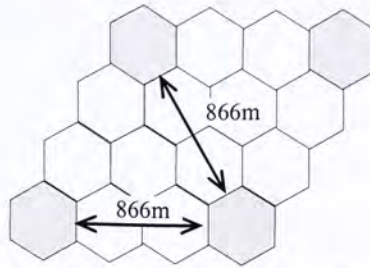
**Figure 4-1: Stations may not interfere with each other
in a 4-by-4 multi-cell WLAN**

= 250m (shown in Figure 3-1). The corresponding maximum IR is therefore

$IR_{max} = 1.78 \times 250m = 445m$. In Figure 4-1, the distance between any two points

of two different shaded areas is more than IR_{max}. Therefore, there is no edge

between vertices of different shaded cells, and a VoIP session in one shaded cell can

transmit simultaneously with a session in another shaded cell.

Since two or more cliques with the maximum size can potentially be formed. This

explains why the total number of VoIP sessions that can be supported in an 802.11b

multi-cell WLAN exceeds 12 and that in an 802.11g multi-cell WLAN exceeds 60

(refer to the average capacities of different multi-cell topologies in Table 3-1).

From Table 3-1, we find more VoIP sessions can be supported when more WLAN

cells are added (D increases). As when D increases, more vertices (VoIP sessions)

have no edge among them, they belong to the different maximal cliques [18]. But

obviously, each maximal clique covers more than one cell, so there are only a few

VoIP sessions can be supported per AP (1.63 VoIP sessions in 5-by-5 802.11b

WLAN). Therefore, to increase the VoIP capacity over multiple WLANs, we need to

find the clique size in the corresponding conflict graph. Hence, we can pack VoIP

23

sessions (vertices) closely.

From the clique analysis above, we know that for supporting VoIP traffic over multiple WLANs, there exists a maximum clique size (e.g. 12 for 802.11b and 60 for 802.11g) which cannot be exceeded. Based on this observation, we can have a clique-based call admission control to increase the capacity of VoIP over multiple WLANs, as discussed in the following sections.

4.3 Clique-Based Call Admission Control Algorithm

4.3.1 Algorithm Description

The ability to predict whether a new VoIP session can be admitted without causing performance problem is important in call admission control. Previous work [2, 17] shows that an additional VoIP session to a single-cell WLAN which already reached the maximum capacity can degrade the performance of all other existing VoIP sessions. This is also the case in multi-cell WLANs. In the 802.11b 2-by-2 network (in which the maximum capacity is around 12.3 as shown in Table 3-1), for example, if there are 14 VoIP sessions, three of them cannot fulfill the loss-rate requirement. That means only 11 sessions can be supported with acceptable performance, as opposed to the 12 sessions that can be supported when there are exactly 12 sessions in the 2-by-2, 4-cell WLAN.

The call admission control schemes proposed in the previous work [2, 17, 45] are for VoIP over single WLAN, the interference from other VoIP sessions of neighboring WLANs was not taken into account. Here we consider a call admission control for VoIP over multiple WLANs. We consider a call admission control mechanism based
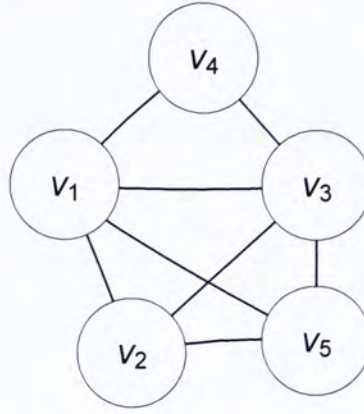
Figure 4-2: An example of a conflict graph

on the clique size of the conflict graph. Let E_{v_i} be the set of vertices with which

vertex v_i has an edge. Let K_{v_i} be the set of all cliques $C_{v_i,x}$ to which v_i

belongs, where $1 \leq x \leq |K_{v_i}|$, $|K_{v_i}|$ is the total number of cliques in K_{v_i}. Any pair of

cliques in K_{v_i} must satisfy (4) below so that all cliques in K_{v_i} are "maximal" and

not contained in another clique [18]. As defined in (5), m_{v_i} is the size of the largest

clique in K_{v_i}.

$$C_{v_i,x} \not\subset C_{v_i,y}, \quad x \neq y, \quad 1 \leq x, y \leq |K_{v_i}| \qquad (4)$$

$$m_{v_i} = \max_x |C_{v_i,x}| \qquad (5)$$

Figure 4-2 gives an example of a conflict graph, where vertex v_1 has the following

parameters.

$E_{v_1} = \{v_2, v_3, v_4, v_5\}$

$K_{v_1} = \{\{v_1, v_2, v_3, v_5\}, \{v_1, v_3, v_4\}\}, \quad |K_{v_1}| = 2$

i.e., $C_{v_1,1} = \{v_1, v_2, v_3, v_5\}, C_{v_1,2} = \{v_1, v_3, v_4\}$

$m_{v_1} = 4$

Algorithm I

Procedure A
Keep a copy of the state (K_{v_j}, m_{v_j}) for all existing v_j;
Perform Procedure B;

Procedure B
For each $v_j \in E_{v_i}$ {
    For each $C_{v_j,x} \in K_{v_j}$ {
        If $C_{v_j,x} \subset E_{v_i}$
            then add v_i to $C_{v_j,x}$;
        else
            add $\{C_{v_j,x} \cap E_{v_i}, v_i\}$ to K_{v_j};
    }
    $K_{v_j} = \text{NO\_REDUNDANCY}(K_{v_j})$;
    Update m_{v_j};

    If $m_{v_j} > C_{\max}$,
        then reject v_i;
        Revert the state using the copy stored in Procedure A;
        Break out of Procedure B, and the algorithm is terminated;
} // *All $v_j \in E_{v_i}$ have been looked at if the algorithm comes to this point*
Perform Procedure C;

Procedure C
v_i is admitted;
$K_{v_i} = \varnothing$;
For each $v_j \in E_{v_i}$ {
    If $v_i \in C_{v_j,x}$
        then $C_{v_i,x} = C_{v_j,x}$,
            $K_{v_i} = K_{v_i} \cup C_{v_i,x}$;
}
$K_{v_i} = \text{NO\_REDUNDANCY}(K_{v_i})$;
Compute m_{v_i};

The pseudo code of the admission control algorithm is given in Algorithm I. There

are three procedures in the algorithm: Procedures A, B and C. When there is a new

call request (i.e., a new vertex v_i (VoIP session) wants to be added), Procedure A

is first executed, wherein a copy of the state $(K_{v_j}, m_{v_j}) \; \forall \; v_j$ is first saved in case

the admission of v_i fails and we need to revert to the original state later. After

that, Procedure B is executed. Procedure B updates the state (K_{v_j}, m_{v_j}) assuming

the addition of v_i. To satisfy (4), a function call $NO\_REDUNDANCY(K_{v_j})$ is

made. Algorithm II gives the pseudo code of $NO\_REDUNDANCY(K_{v_k})$. During

the updating, Procedure B continually checks to see if a pre-determined maximum

clique size C_{max} is exceeded so as not to violate the loss-rate requirement. If so, the

algorithm is terminated and v_i is rejected; in which case the state saved in

Procedure A is restored.

If Procedure B successfully runs to the end without the C_{max} being exceeded,

Procedure C is executed. Procedure C admits the new vertex v_i and

calculates (K_{v_i}, m_{v_i}).

4.3.2 Algorithm Performance Evaluation

We have performed an experiment in MATLAB to measure the execution time of the

Algorithm II

```
NO_REDUNDANCY (K_{v_k}) {
    For each pair  C_{v_k,x} ∈ K_{v_k} and C_{v_k,y} ∈ K_{v_k} , x ≠ y {
        If  C_{v_k,x} ⊂ C_{v_k,y}
            then delete C_{v_k,x} ;
    }
    Return  (K_{v_k}) ;
}
```

call admission control algorithm. In the experiment, we use the 5-by-5 multi-cell

topology setting in Section 3.1. We assume 802.11b and apply the algorithm to find

which VoIP sessions out of a total of 300 (12 x 25) randomly placed (with uniform

distribution) potential sessions can be admitted in a 5-by-5 multi-cell WLAN with

the C_{max} constraint on the largest clique size. We start with an empty network, and

call admission is requested one by one until all the 300 potential sessions have

attempted. Unlike the Simplistic Call Admission Scheme earlier, here when a

session is rejected, the call admission scheme continues to consider a next session if

all the 300 sessions have not been exhausted. We ran several sets of experiments for

different random node distributions in a 5-by-5 WLAN. We use an ordinary personal

computer with 3.2GHz CPU and 1G RAM to perform the experiment. The results

for C_{max}= 8 and 12 are shown in Table 4-1. The total runtime is the total time needed

**Table 4-1: Experiment Results of Applying the Admission
Control Algorithm on 5-by-5 Multi-Cell WLAN**

C_{max}	Total Runtime (s)	Average No. of Sessions Admitted	Average Runtime (s)
8	48.6	62.0	0.160
12	112.1	70.4	0.374

for the algorithm to go through all the 300 VoIP sessions. The average runtime is the

time the algorithm needed to admit or reject a call (Total runtime / 300) in our

experimental setting. We see that although the general clique problem is

NP-complete, the execution time of our algorithm on the conflict graph that models

802.11 networks is actually acceptable.

Based on the call admission results in MATLAB, we then used NS2 to verify

whether the admitted calls meet the maximum 3% packet-loss rate requirement in

the simulation. From Table 4-1, we find that when C_{max} is 8, the average number of

VoIP sessions admitted by our admission control algorithm is 62.0. This is the average number of five runs. We incorporated the corresponding sets of admitted VoIP sessions in five different runs of NS2 simulation. In each run, all the admitted VoIP sessions can meet our packet-loss rate requirement.

However, if we instead use the corresponding sets of the admitted VoIP sessions when C_{max} is 12 in the NS2 simulations, nearly one third of them cannot meet the loss requirement. It is interesting that for the large-scale multi-cell case, the maximum clique size that should be imposed is 8 rather than 12 (recall that 12 is the maximum clique size in the single-cell topology in 802.11b is assumed) if loss-rate requirement is to be satisfied. This is perhaps due to the interaction and "coupling" among different cliques caused by the 802.11 MAC protocol. In other words, 802.11 MAC may not achieve perfect scheduling in which the airtime usage within each clique is 100% tightly packed. This motivates us to explore the use of timeslot scheduling over the basic CSMA 802.11 MAC in Chapter 5 for performance improvement.

With $C_{max} = 8$, the 5-by-5 multi-cell WLAN can support 2.48 sessions (62.0/25) per AP, yielding a 52.1% improvement over the Simplistic Call Admission Scheme in Chapter 3.

4.3.3 Clique-Based Admission Control in Three-Frequency-Channel WLAN

So far our discussion mainly focuses on the per-AP VoIP capacity over single-frequency-channel WLAN. In this subsection, we explore the impact of multiple frequency channels on VoIP capacity over multiple WLANs. As mentioned in Section 3.3, the three orthogonal frequency channels in 802.11b/g are not enough

to isolate the co-channel interference of nearby cells. However, the availability of multiple frequency channels allows us to separate the cells using the same frequency by a longer distance.

Farther separation of cells that use the same frequency leads to less conflict among transmissions of different VoIP sessions (although not eliminating conflicts entirely). Consequently, fewer edges are formed in the corresponding conflict graph. Consider the multi-cell topology in Figure 4-3, where we apply the three frequency-channel assignment (like Figure 3-3). In Figure 4-3, the shaded cells use the same frequency channel, while the un-shaded cells use the other two frequency channels. Although the size of the topology in Figure 4-3 is comparable to the 5-by-5, 25-cell WLAN we described in previous sections, three frequency channels help to reduce conflicts and increase the number of VoIP sessions that can be supported by each AP. The NS2 simulation shows that applying the clique-based admission control in this three frequency-channel layout can boost the per-AP capacity to 7.39 VoIP sessions. It is 2.98 times of the per-AP capacity in 5-by-5, 25-cell WLAN where single-frequency channel is used (2.48 sessions per AP).

**Figure 4-3: 3-frequency-channel assignment
is applied on multiple WLANs**

Another dimension to improve the dismal VoIP capacity over multiple WLANs is to reduce the edge formation of the corresponding conflict graph by modifying 802.11 MAC protocols. The edges are formed according to the *CSRange* and *IR* (conditions (i) and (ii) in Section 4.1 respectively) of the nodes (can be wireless client station or AP) in multi-cell WLAN. As the *CSRange* value in the standard 802.11 MAC is a fixed value and is not set "optimally", there are exposed nodes (EN) [19]. To reduce the edge, we may try to apply an advanced MAC protocol, called MP [20] which we proposed previously, to remove the EN in the network. However, although MP effectively increases network throughput when data packet size is large, it does not increase the VoIP capacity effectively due to its large packet header overhead. On the other hand, a so-call Receiver Restart (RS) mode in 802.11 MAC (available in some products, for example, Atheros Chip) can also reduce edges of conflict graph by alleviating HN. In doing so, the VoIP capacity can be increased [10]. However, RS mode alone cannot remove HN completely. In the next chapter, we explore time division on 802.11 MAC which can eliminate all HN and alleviate EN. The VoIP capacity over multiple WLAN, therefore, can be potentially increased significantly. We relegate the discussion of MP and RS mode to Appendices 1 and 2 respectively.

Chapter 5

Time Division Multiple Access (TDMA) on IEEE 802.11 MAC

So far we have learned that there is a significant capacity penalty when we move from the single-cell WLAN scenario to the multi-cell WLAN scenario. We have also learned that the extremely low VoIP capacity over multiple WLANs is due to the mutual interference from neighboring cells, and such mutual interference cannot be completely isolated even with careful frequency channel assignment. Although IEEE 802.11e has been standardized recently to support QoS in WLAN [21], it only focuses on the single-cell situation.

In this chapter, we explore adding the time-division approach to the basic 802.11 CSMA protocol. We show that the integrated timed-division-CSMA approach can potentially increase the VoIP capacity over multiple WLANs quite significantly. Our discussion focuses on integrating time-division approach into the 802.11 context in multiple WLANs. Some previous work has also considered Time Division Multiple Access (TDMA) MAC in single WLAN. However, their focus is on a single WLAN [22-25] and where CSMA is replaced entirely by TDMA [26-28]. For VoIP applications, each transmission consists of a very small packet, and such "fine" TDMA requires tight synchronization among the stations, which can in turn cause throughput degradation.

In this chapter, our primary focus is on the principle of "coarse" time division, in which a relatively large timeslot is allocated to a group of stations. The stations of

the same timeslot then contend channel access using the original 802.11 CSMA scheme. We (i) lay out and investigate a graph-theoretic problem formulation that captures the principle of integrating coarse time division with CSMA in Section 5.1; and (ii) provide a preliminary feasibility investigation of the approach within the context of 802.11 in Section 5.2.

5.1 Coarse-Grained Time-Division Multiple Access (CTDMA)

In Section 3.3, we have discussed 3-frequency-channel assignment in 802.11b WLAN (see Figure 3-3) and argued that frequency-channel assignment alone cannot completely isolate co-channel interference. In Section 4.3.3, although applying the clique-based call admission control can boost per-AP VoIP capacity in 3-frequency-channel WLAN, the co-channel interference from different cells is still not isolated entirely. The goal of Coarse-Grained Time-Division Multiple Access (CTDMA) is to remove such co-channel interference. In particular, two stations in different cells that may interfere with each other could be restricted to transmitting at different times.

5.1.1 Basic Ideas of CTDMA

We first present the concept with the *simplified* scenario depicted in Figure 5-1. In Figure 5-1, in addition to the 3-frequency-channel assignment, we divide each cell into six sectors and assign a distinct timeslot to each sector. The shaded cells use the same frequency channel, and the stations within each sector use the same timeslot; the number in each sector indexes the timeslot assigned to that particular sector. The frequency and timeslot assignments in Figure 5-1 are such that different sectors do not interfere with each other because they are either active in different timeslots, in cells of different frequencies, or sufficiently far apart from each other. This allows us
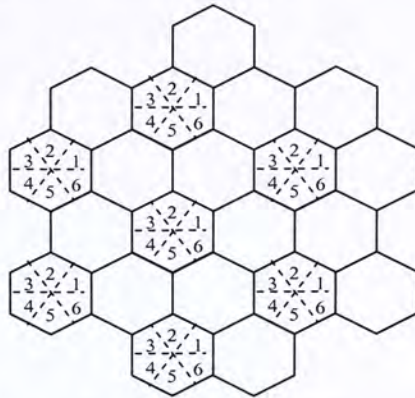
Figure 5-1: Timeslot assignment in addition to 3-frequency-channel assignment in multiple WLANs

to shorten the carrier sensing range (*CSRange*) of the stations to d_{max}, the distance from the AP located at the center of each cell to the farthest corner in the cell. The nearest station with the same timeslot assignment in neighboring cells is at least $2d_{max}$ away, which is larger than both the *CSRange* and maximum *IR* defined in (3). Therefore, the co-channel interference from neighboring cells is completely isolated. Note that within each sector (timeslot), there may still be multiple stations, and the original 802.11 CSMA scheme is used to coordinate transmission among these stations. In the best-case scenario, the *VoIP capacity per AP* in multiple WLANs can be the same as that in the single isolated WLAN case. Consider 802.11b, if each sector has two stations, then we can have a total of 12 VoIP sessions per AP.

Although the sectorized cells in Figure 5-1 illustrate the concept of CTDMA, it has two implementation difficulties: 1) timeslot assignment requires the knowledge of the locations of the individual stations in order to sectorize them effectively; 2) if the stations are not evenly distributed across the sectors, then it will not be as effective as the best-case scenario mentioned above. In the following subsections, we present

a graph model of CTDMA to solve these problems. The graph model presented also gives a framework for the analysis of CTDMA (a topic for future study).

Before going into the graph model of CTDMA, we define CTDMA as follows.

Definition 2: Coarse-Grained Time-Division Multiple Access (CTDMA)

In CTDMA, m frequency channels and n timeslots are assigned to the VoIP sessions. In each cell, at most k VoIP sessions are active in each timeslot, where $k = \lfloor C_{AP\_1} / n \rfloor$, and C_{AP_1} is the average per-AP capacity in a single isolated WLAN.

5.1.2   Conflict Graph Modeling of CTDMA

According to the Definition 2, the parameter m in CTDMA is the number orthogonal frequency channels available. For example, $m = 3$ in 802.11b and 802.11g (for 802.11a, $m = 12$). On the other hand, n is the number of timeslots that is defined by users, and is independent of m. The largest value of n cannot exceed C_{AP_1} of the corresponding 802.11 standards. "Virtual channels" with different frequency-time slot combinations are orthogonal in that VoIP sessions assigned to different virtual channels will not interfere with each other. So, either increasing n or m can increase the number of independent virtual channels. If $n = 6$, then $k = 2$ in 802.11b, and $k = 10$ in 802.11g, since the respective C_{AP_1} are 12 and 60. We will look at the system performance as a function of n shortly. First, we formulate the corresponding graph-theoretic coloring problem. For CTDMA, a modified construction of the conflict graph, as well as a modified coloring problem, is needed to reflect the problem being tackled, as detailed below.

Instead of pre-assigning the three frequency channels as in Figure 5-1, we now

integrate the frequency channel assignment and timeslot assignment into a single framework under CTDMA, as follows. In the CTDMA conflict-graph model, we use two layers of coloring. The first-layer colors represent frequency channels and the second-layer colors represent timeslots. The first-layer coloring is applied at the cell level while the second layer coloring is applied at the station (vertex) level. In the following, we first state the constraints of our coloring problem under the context of 802.11, and then describe how to capture the constraints in the conflict graph.

In a conflict graph, vertices usually correspond to links. However, in an infrastructure network, since all links have the AP at one end, for convenience we associate vertices with the client stations in the following:

Constraint 1: The number of available first-layer colors is m, and the number of available second-layer colors is n (see Definition 2)

Constraint 2: All vertices associated with the same AP (within the same cell) must have the same first-layer color.

Constraint 3: Within a cell, there can be at most k vertices assigned with the same second-layer color. Furthermore, the vertices assigned the same second-layer color in a cell must be within the *CSRange* of each other.

For vertices within the same cell, it is obvious that the associated stations cannot transmit together since one end of the links is always the AP. The issue for vertices within the same cell is that whether the *CSRange* of vertices (clients) can cover each other, hence Constraint 3.

Constraint 4: Consider two vertices of different cells, v_i and v_j. They conflict with each other and must be assigned different (first-layer-color, second-layer-color) if one or more of the following inequalities below are satisfied:

$$CSRange \geq \min(d_{v_i,v_j}, d_{v_i,v_j'}, d_{v_i',v_j}, d_{v_i',v_j'}) \tag{6}$$

$$
\begin{aligned}
IR_{v_i} &> \min(d_{v_i,v_j}, d_{v_i,v_j'}) \\
IR_{v_i'} &> \min(d_{v_i',v_j}, d_{v_i',v_j'}) \\
IR_{v_j} &> \min(d_{v_i,v_j}, d_{v_i',v_j}) \\
IR_{v_j'} &> \min(d_{v_i,v_j'}, d_{v_i',v_j'})
\end{aligned}
\tag{7}
$$

where v_i' and v_j' are the corresponding APs that v_i and v_j associated respectively. Note that both (6) and (7) describe the conditions under which simultaneous transmissions are not possible. However, there is a subtlety. Inequalities (7) capture the conditions that will lead to collisions. Inequality (6), on the other hand, only says that the CSMA mechanism will prevent the stations from transmitting together – that is, strictly speaking, if satisfied, the stations could still be assigned the same color combination, and the CSMA mechanism simply prevents simultaneous transmissions. Constraint 4, however, disallows that as a design choice to simplify things. The reasons are as follows: (i) If different color combinations are used whenever (6) is satisfied for two vertices in different cells, then CSMA in different cells will then be decoupled in each of the timeslots under CTDMA, obviating the need for inter-cell CSMA. (ii) When combined with constraint (7), the performance-degrading hidden-node phenomenon [15] across cells will not arise. Indeed, when constraints (6) and (7) are imposed on CTDMA coloring, we may decrease *CSRange* to only meet the need of intra-cell CSMA, and there is no need

for *CSRange* to be large enough to ensure proper CSMA operation across cells. This has the advantage of reducing exposed nodes (EN) across cells [19], hence increasing spatial re-use. In the next subsection, we will explore the "optimal" value for *CSRange* through simulations.

Capturing Constraints 2 to 4 in Conflict Graph

To capture constraint 2, we could assign an AP_ID to the vertices in accordance with the APs to which they associate. Vertices with the same AP_ID must be given the same first-layer color.

For constraints 3 and 4, an edge between two vertices mean they must be assigned different (first-layer color, second- layer color) combination.

To capture constraint 3, there is an edge between two vertices v_i and v_j of the same cell if

$$d_{v_i, v_j} > CSRange \qquad (8)$$

Two vertices that are within the *CSRange* of each other could be assigned the same or different second-layer color. However, there can be at most k vertices with the same second-layer color within a cell.

Constraint 4 can be captured by drawing an edge between two vertices of different AP_ID if there is a conflict relationship under inequalities (6) and (7). To avoid confusion, it is worth emphasizing again that between vertices of different AP_ID (from different cells), we use (6) and (7) for the edge formation criteria. For vertices

of the same cell, we use (8) for the edge formation criteria.

A formulation of the CTDMA problem is as follows:

2-Color Assignment Problem: Assign (first-layer color, second-layer color) to the vertices subject to constraints 1 to 4 such that the total number of vertices successfully colored is maximized.

Figure 5-2 illustrates the idea of CTDMA. APs (triangles) are at the center of the cells, client stations (circles) in the same cell are associated with the same AP. The
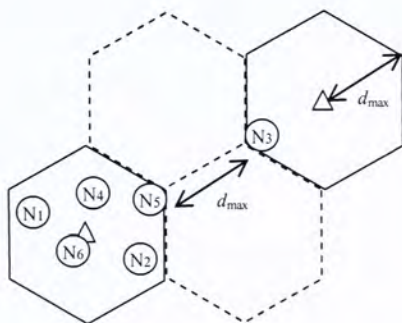

Figure 5-2: A topology of VoIP over multiple WLANs with 3-channel assignment

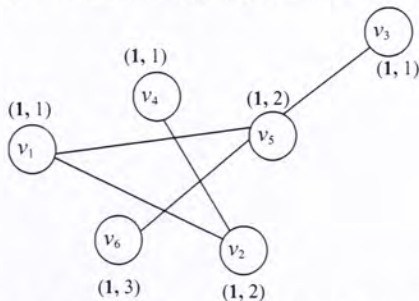solid-line cells use the same frequency channel while the dotted-line cells use the

Figure 5-3: A conflict graph with first-layer and second-layer coloring for network in Figure 5-2.

other two frequency channels. For simplicity, we assume the standard 3-frequency-channel assignment (as shown in Figure 5-1) here for the frequency channel assignment in CTDMA. It is worth noting that this standard 3-frequency-channel assignment is not a must for CTDMA. If we do not have such assumption, we would add AP_IDs to the vertices represent the clients. The clients in the same cell have the same AP_ID. According to Constraint 2, vertices represent clients N_1, N_2, N_4, N_5 and N_6 must have the same first-layer color, while the vertex represents N_3 has freedom to choose a different first-layer color. However, with the assumption of standard 3-frequency-channel assignment, the vertices represent clients N_1 to N_6 all have the same first-layer color. Furthermore, we assume 802.11b and $n = 6$ (which implies $k = 2$ given a capacity of 12 VoIP sessions per cell) and $CSRange = d_{max}$. Once the first-layer colors are assigned, the second-layer coloring is described as follows.

Figure 5-3 shows the corresponding conflict graph together with the coloring. The bold numbers in parentheses beside the vertices are the first-layer colors while the other numbers are the second-layer colors. Readers are reminded that this conflict graph only captures the constraints for the second-layer coloring (AP_ID is omitted here), and for simplicity, we pre-assign the first-layer colors to the vertices (in this example, all the vertices have the same first-layer color as the standard 3-frequency-channel coloring like in Figure 5-1 is used). According to constraint 3, for second-layer coloring, v_1 and v_4 (which represent N_1 and N_4 respectively) are assigned COLOR1, v_2 and v_5 (which represent N_2 and N_5 respectively) are assigned COLOR2, and v_6 (which represents N_6) is assigned COLOR3. N_3 and N_5 may interfere with each other under (6) and (7), so an edge is drawn between v_3 and v_5. According to constraint 4, the two vertices must be assigned with different color

(first-layer color, second-layer color): in Figure 5-3, COLOR1 is assigned to v_3 and COLOR2 is assigned to v_5.

5.1.3 Parameter values in CTDMA

An important parameter in CTDMA is n, the number of the timeslots (second-layer colors) available for the system. From Definition 2, k, the number of VoIP sessions that can be active in the same timeslot in a cell is set accordingly to n. In the above example, we set $n = 6$ and $k = 2$. The value of n directly affects the number of vertices that can be successfully colored. A larger n (i.e. a smaller k) means more finely-divided timeslots. In the extreme case, $k = 1$ ($n = C_{AP\_1}$, i.e. $n = 12$ for 802.11b and $n = 60$ for 11g), which is a pure TDMA scheme. In this case, every VoIP session in a cell is assigned a distinct timeslot. Hence, no carrier sensing is required for accessing the medium. From the graph-theoretic coloring viewpoint, fine TDMA as such would allow us to increase the number of vertices successfully colored in the two-layer-color assignment problem defined above. However, fine TDMA has an implementation cost not captured in the coloring problem – namely, there is the need for a "guard time" as we switch from slot to slot (for synchronization purpose). This implementation issue will be further discussed in the next section. For the time being, suffice it to say that we are interested in making k as large as possible (i.e. making n as small as possible) while retaining the performance results of the case where k is set to 1.

Another important parameter in CTDMA is *CSRange*. As mentioned before, CTDMA allows us to decrease *CSRange* and the carrier sensing mechanism is only within a cell. This eliminates the EN (exposed-node) problem among different cells that runs counter to effective spatial re-use. However, if the *CSRange* is too small, a

client may only carrier-sense few other client stations within the cell. According to constraint 3 (and inequality (8)), small *CSRange* may cause more intra-cell edges in the conflict graph that restrict coloring freedom.

For illustration, let us first consider setting *CSRange* to be the sector diameter, as described below. Each cell is divided into n sectors in a fashion that generalizes Figure 5-1. *CSRange* could be set to cover the maximum distance between any two points within a sector. Let us refer to the maximum distance as the "diameter" of the sector. For example, if 802.11b is assumed, $C_{AP\_1} = 12$. For $n = 12, 6, 4, 3, 2,$ and 1, the corresponding *CSRange* could be set as shown in Table 5-1. From Table 5-1, we also show the corresponding values of k according to Definition 2. If 802.11g is assumed, the same set of *CSRange* values should be used if $n = 60, 6, 4, 3, 2$ and 1 (as in 802.11g, $C_{AP\_1} = 60$).

The sector-diameter is a "worst-case" setting in the sense that it assumes that there exist actually two stations at the extreme corners of a sector that define the diameter, which is rarely the case. It would therefore be of interest to explore tuning the *CSRange* to maximize the number of vertices can be successfully colored in the conflict graph. We present the simulation results based on the sector-diameter settings as well as "smaller-than-sector-diameter" settings below.

We first show the results of sector-diameter settings. Based on the parameters in

Table 5-1: Values of n, k and Corresponding *CSRange* in 802.11b

n	12	6	4	3	2	1
k	1	2	3	4	6	12
CSRange	0	d_{max}	$\frac{\sqrt{7}}{2}d_{max}$	$\sqrt{3}d_{max}$	$\frac{\sqrt{13}}{2}d_{max}$	$2d_{max}$

Table 5-1, we have performed MATLAB experiments assuming 802.11b (C_{AP_1} = 12) and 802.11g (C_{AP_1} = 60). For simplicity, the standard 3-frequency-channel assignment is assumed. Since the first-layer colors are pre-fixed in this experiment, only second-layer coloring (time-slot assignment) is considered. We use hexagonal cells to model WLAN (like the one in Figure 5-1), and 12 (for 802.11b) or 60 (for 802.11g) wireless client stations are randomly placed inside each cell with uniform distribution.

We use a heuristic algorithm of Welsh and Powell [29] to color the conflict graph. We add our coloring constraints 1 to 4 to tailor the algorithm to CTMDA. The algorithm of Welsh and Powell does not give optimal graph coloring in general, but the effect of n is already quite pronounced even with the simple heuristic.

Figures 5-4 and 5-5 respectively show the percentages of vertices that can be colored when C_{AP_1} = 12 and C_{AP_1} = 60. In the experiment, *CSRange* changes accordingly to n as dictated by Table 5-1. For each n, we ran five experiments with different node distributions. In the figures, circles are the average percentage of successfully colored vertices. In general, as n increases, more vertices can be successfully colored. Although not shown in the figures, the two cases for n = 12 in 802.11b and n = 60 in 802.11g have 100% of their vertices successfully colored in all runs of our experiments. But even for n as small as 3 or 4, the performance of CTDMA is already very good (100% of vertices are colored in 802.11b, while more than 95% of vertices are colored in 802.11g). With smaller n, the overhead of guard-time for switching between timeslots can be reduced (to be elaborated shortly) and n = 3 or 4 may offer the best design tradeoff.
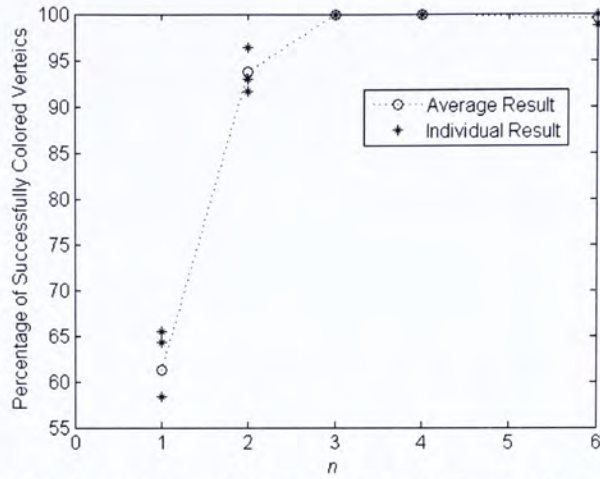
Figure 5-4: Percentage of colored vertices when *CSRange* is set as "sector-diameter" and $C_{AP\_1}=12$ (802.11b)
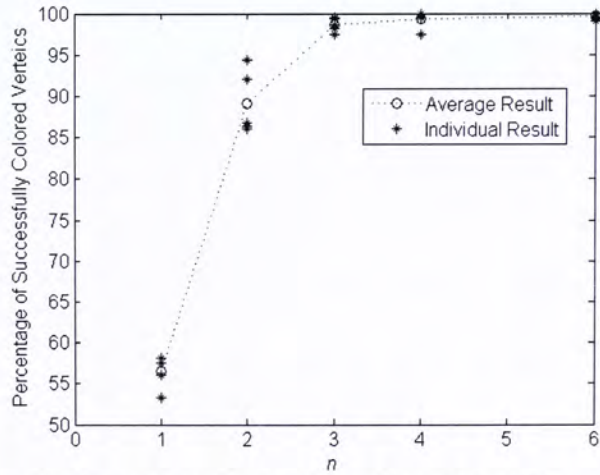
Figure 5-5: Percentage of colored vertices when *CSRange* is set as "sector-diameter" and $C_{AP\_1}=60$ (802.11g)

In the next set of experiments, for each run, we set a fixed *CSRange* for all values of *n*. Across different runs, we vary *CSRange*. Figures 5-6 and 5-7 show the average percentage of successfully colored vertices as a function of *n* under different fixed *CSRange*. We find that when *CSRange* is d_{max}, the overall system performance is poor (especially when *n* has small values) because many edges are formed within a
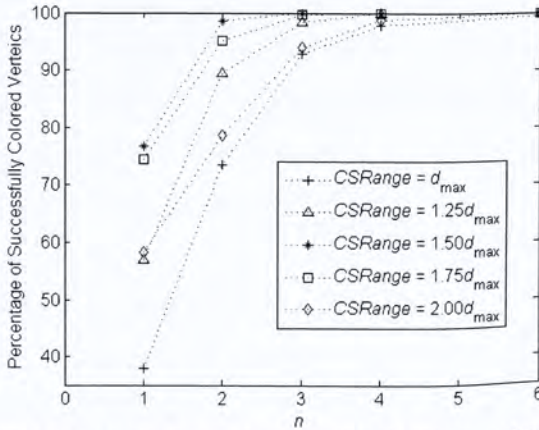
Figure 5-6: Average percentage of colored vertices as *CSRange* changes when C_{AP_1}=12 (802.11b)
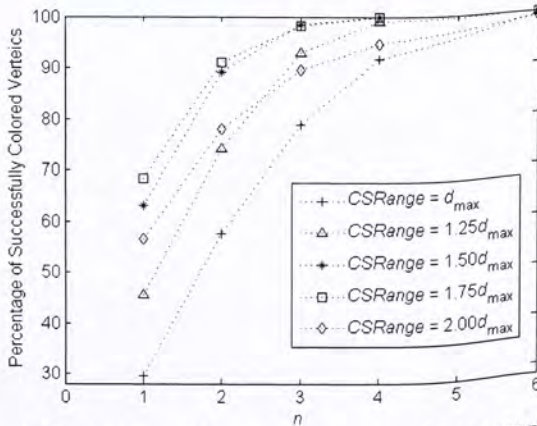
Figure 5-7: Average percentage of colored vertices as *CSRange* changes when C_{AP_1}=60 (802.11g)

cell (according to (8)).

As *CSRange* increases, the overall system performance improves. But beyond certain point (e.g., $1.5d_{max}$ in the figures), the overall system performance drops again. This phenomenon reveals the tradeoff between intra-cell optimality and inter-cell optimality. When *CSRange* is too large, say $2d_{max}$, many edges are formed between vertices of different cells (according to (6)), leading to an increase of exposed nodes. Through experimentation, we find the "optimal" *CSRange* which yields the "best" system performance in around $1.637d_{max}$. Indeed, we could use this setting for different *n* values with reasonably good results (see Table 5-2).

Our experiment results show that CTDMA can generally color large portions (over 90%) of the vertices of the conflict graph when $n \geq 3$ for both 802.11b and 802.11g. The performance can be even better when appropriate ("optimal") *CSRange* is set. By contrast, without CTDMA, and with 3-frequency-channel assignment alone ($n = 1$), we find that only around 60% of the total capacity can be utilized.

CTDMA is closely related to the channel assignment problem which was widely studied. Ref. [46] has even proposed a unified framework for the study of assignment problems. But the two layers of coloring (frequency and timeslot) in

Table 5-2: System Performance for CSRange = $1.637d_{max}$

n	1	2	3	4	6	$C_{AP\ 1}$
% vertices success- fully colored in 802.11b	80.0	98.6	100	100	100	100
% vertices success- fully colored in 802.11g	69.8	93.0	99.6	100	100	100

CTDMA and its application to increase VoIP capacity over multiple WLANs are new. So, the unified framework and algorithm for channel assignment problem in [46] cannot be directly applied to CTDMA either. By the above heuristics, we preliminarily evaluate the potential benefit of CTDMA for increasing VoIP capacity over multiple WLANs. More formal analyses are needed in future work.

5.2 Possible Realization of TDMA on 802.11 Standards

Most of the previous work [23-28] considered proprietary protocols for implementing TDMA on wireless networks. Our focus here is to implement timeslot assignment within the framework of the IEEE 802.11 standard. A most critical issue is how to realize the concept of "timeslot" within the 802.11 CSMA structure. A possibility is to make use of the "sleeping mode" in 802.11, which was originally designed for power conservation purposes. In the sleeping mode, beacon frames are used for synchronization. Accordingly, in CTDMA, all stations could wake up around the beacon time for synchronization. As illustrated in Figure 5-8, in CTDMA, within each beacon interval (*BI*) between the *end* of a beacon and the *beginning* of the next beacon, the time is divided to C frames (cycles), each of duration ΔT. Within each frame, there are n timeslots, each of duration Δt. A VoIP stream
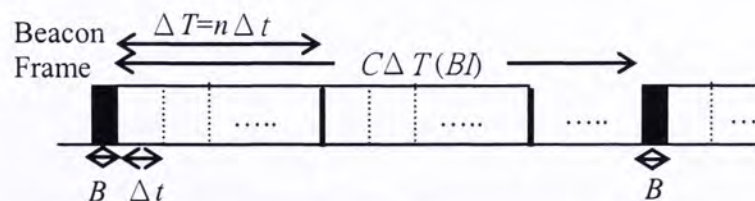

Figure 5-8: Frame structure of CTDMA when it is implemented using 802.11 sleeping mode

47

transmits one VoIP packet in each frame. The offset from the end of the beacon to the beginning of the ith frame is $(i-1)\Delta T$. A station that has been assigned timeslot j is to be awake within a BI only during the time intervals specified by $[(i-1)\Delta T + (j-1)\Delta t, \ (i-1)\Delta T + j\Delta t)$, $i = 1, 2, ..., C$. Other than these time intervals and the beacon time, the station sleeps.

Guard Time Overhead in CTDMA

The guard time should be set to the duration of one VoIP packet. That is, no packet transmission should be initiated within the current timeslot when the beginning of the next timeslot is only a guard time away. This is to ensure packet transmission will not straddle across two timeslots. Let $r_{\Delta t}$ be the *maximum* number of VoIP packets (including the CSMA overhead) that could be transmitted and received within each timeslot by all VoIP sessions which are active in that particular timeslot. Then,

$$r_{\Delta t} = 2 \times \frac{R_{VoIP}}{10nC} \times C_{AP\_1}$$ (9)

where R_{VoIP} is the number of VoIP packets generated per second in a particular VoIP codec. The factor of 2 is due to each VoIP session having a downstream and an upstream flow. The factor of $1/10$ is due to the default 0.1 s separation time between two beacons. By default, the separation time between two beacons (from the beginning of one beacon to the beginning of the next) is 100ms. The guard time overhead is a constant of one VoIP-packet duration, so that the timeslot efficiency is $(r_{\Delta t} - 1)/r_{\Delta t}$. Thus, smaller $r_{\Delta t}$ gives rise to lower efficiency, which in turn results in lower capacity. From (9), we can see that it is desirable to set n and C as small as possible. From the simulation experiments in the previous subsection; however, we need to make sure that $n \geq 3$ (see Section 5.1.3) so as to make sure most sessions

within the system capacity limit can be admitted. While call admission consideration imposes a limit on how small n can be, the delay budget consideration imposes a limit on how small C can be, as explained below. That is, the factors that bound on the size of n and C are different.

In CTDMA, the maximum delay for a VoIP packet is $\Delta T + B$, where B is the duration of the beacon (see Figure 5-8). To see this maximum delay, let us consider the station being assigned timeslot j. In the worst case, it could generate a packet in the last frame within a BI just slightly after timeslot j ends, thus missing it. The earliest time for the next timeslot j - in the next BI - is $\Delta T + B - \Delta t$ after that. Within this next time slot j, in the worst case, the packet is sent just before the end of the timeslot (due to the CSMA contention with other stations assigned the same time slot). If we assume the packet will be discarded if it fails to be sent out by this time - so as to make way for a newly generated packet from the same VoIP session - the maximum delay is then $\Delta T + B$. Thus,

$$\Delta T + B \leq DB \tag{10}$$

where DB is the delay budget. Since $C\Delta T = BI$ (see Figure 5-8), we have

$$BI / C + B \leq DB => C \geq \frac{BI}{DB - B} \tag{11}$$

Suppose we set a local delay budget of 30ms for VoIP applications [5]. A typical value of B is 0.5ms. With the default separation time between two beacons of 100ms, a beacon interval, BI, is 99.5ms. Hence, the number of frames, C, in a beacon interval, is at least 99.5/29.5 = 3.37. C should be a positive integer as well, so the smallest C is 4.

Assuming $n = 3$, $C = 4$, and GSM 6.10 codec and 802.11b ($R_{VoIP} = 50$, $C_{AP\_1} = 12$), from (9) we find that 90% of capacity is utilized. That is at most $\lfloor 12 \times 90\% \rfloor = 10$ VoIP sessions can be admitted per AP in 802.11b networks. If 802.11g is assumed ($C_{AP\_1} = 60$), 98% of capacity is utilized. That is, 58 VoIP sessions per AP can be admitted in 802.11g networks.

Take 802.11b WLAN as an example, with CTDMA (where three frequency channels are used), the per-AP capacity over multiple WLANs is 10 VoIP sessions. This is a 35.3% improvement over the per-AP capacity of 7.39 sessions for the three-frequency-channel clique-based call admission control strategy (see Section 4.3.3).

Another possibility for implementing the concept of time-division is to use the "polling mechanism" of Point Coordination Function (PCF) [11] to imitate the timeslot assignment in CTDMA. In PCF, traffic is scheduled by the AP, so that no extra guard-time overhead is needed for timeslot switching. If we assume PCF, we could set $n = C_{AP\_1}$ (i.e. $k = 1$) in CTDMA. We refer this setting as Fine-grained Time Division Multiple Access (FTDMA). In PCF, an AP maintains a polling list containing all the wireless stations in its WLAN. In the contention-free period, the AP polls the stations on the polling list one by one, since only one VoIP session is active in each timeslot in a cell in FTDMA. Only the polled station can transmit packets to AP (the downstream packet is attached in the polling packet). The position of a station in the polling list corresponds to the timeslot assigned to the station. In this way, stations which may interfere with each other in adjacent cells will not be polled at the same time.

With FTDMA, the number of vertices successfully colored can be increased. Furthermore, since only one VoIP session is active in each timeslot in a cell, carrier sensing mechanism can be deactivated. Without backoff countdown in contention period, C_{AP_1}, the average per-AP capacity in single isolated WLAN, can be boosted in PCF (in 802.11b, C_{AP_1} increases from 12 to 17, while in 802.11g, C_{AP_1} increases from 60 to over 90). A major concern, however, is that PCF is seldom used in practice and many 802.11 devices do not support it – unlike DCF, the robustness of PFC in field deployment has not been well tested.

The above realization of TDMA is based on the assumption of omni-directional antennas. We may also consider the use of directional antennas or beam-sweeping to realize the time-division in WLAN. If the AP has a directional antenna, then it can sweep the cell in a periodic manner by steering its beam direction. This has the effect of increasing the isolation among different stations. The stations (VoIP sessions) work only if the signal (or beam) of the AP are received. The stations sleep in other time when the AP's antenna sweeps to other areas of the cell. However, tight synchronization between AP of different cells is also required to isolate co-channel interference among different stations. This is deferred to the future studies.

Chapter 6

Coloring Problem in Wireless Networks: A Theoretical Treatment

It is well known that channel assignment problem (CAP) for cellular system is generally solved by graph-coloring algorithm [30]. In Chapter 5, we have discussed how to assign timeslots to VoIP sessions for increasing VoIP capacity over multiple WLANs. In this chapter, we consider a theoretical approach to the coloring problem in wireless networks. In particular, instead of specifically considering IEEE 802.11 networks, we consider the more general setting of assigning orthogonal channels to links. Therefore, we only take Interference Range (*IR*) (as defined by (3)) as the edge formation criterion for the conflict graph of a wireless network. We assume that there is an underlying mechanism to effect this assignment and schedule the transmissions. The underlying mechanism could be an "ideal" centralized coordinator, in which case the assignment would be perfect in accordance with the solution of the coloring problem; or the carrier-sensing mechanism of 802.11, in which case the solution of the coloring problem only serves as a performance bound (since 802.11 may not schedule transmissions perfectly according to the solution of the coloring problem). In all cases, consideration of the coloring problem gives us an idea of the best that can de done.

We prove that for a one-dimensional linear wireless network, the maximum number of colors (channels, e.g. timeslots, frequency- channels) required is the same as the maximum clique size of its corresponding conflict graph. However, the problem becomes much more complicated when two-dimensional wireless networks are considered. In this chapter, we also give a preliminary discussion on the coloring
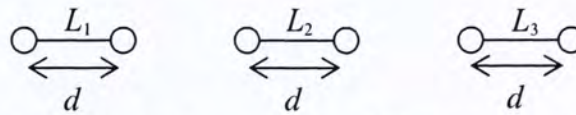
Figure 6-1: An example of linear network with same link length

problem in a two-dimensional wireless network and its implication to the VoIP over multiple WLANs.

6.1 Coloring of One-Dimensional Linear Network

6.1.1   Network with Same Link Length

We first consider a simple case, in which all links in the linear network have the same link length.

Figure 6-1 shows a simple example of a linear network with same link length. In the figure, all three links, L_1, L_2 and L_3 have the same link distance, d. It should be noted that the links in Figure 6-1 do not overlap. The definition of one-dimensional linear network (see Section 6.1.2) does not have this constraint. i.e. links can overlap, and a node can be shared by two or more links.

We can construct a corresponding conflict graph of the one-dimensional linear network with same link length.

It is well known that an interval graph (a graph in which the vertices are represented by a set of intervals on the real line and an edge between a pair of vertices corresponds to that pair of intervals intersect [31]) is a perfect graph. A perfect graph is a graph in which the chromatic number $\chi(H)$ of every induced subgraph H, equals to the clique number $\omega(H)$ of that subgraph [32].

Corollary 1: *If G is the conflict graph of a linear network with the same link length, then* $\chi(G) = \omega(G)$.

Proof: Consider a linear network with same link length. Suppose there are a total of n links. We denote the node in the left hand side position of a link L_i as x_i and the right hand side position of L_i as y_i, so that $y_i \geq x_i$, where $1 \leq i \leq n$. We order the links from left to right. In addition, we use d to represent the length of L_i for all i (all links have the same link length). Let the interval $[x_i, z_i]$, be the vertex v_i. z_i is defined in (12).

$$z_i = y_i + (1 + \Delta)d \qquad (12)$$

Therefore, a corresponding interval graph is constructed. It is clear that the interval graph G', constructed out of these intervals, is the same as the conflict graph, G. $\chi(G') = \omega(G')$, thus $\chi(G) = \omega(G)$.

Q.E.D

Corollary 1 implies that for a linear network with same link length, if channel assignment is applied, the maximum number of channels needed could be as same as the maximum clique size. If the links are not overlapped, it is obvious to figure out that the maximum clique size is three. Therefore, three channels are enough to isolate interference relationship among the links.

6.1.2 Network with Variable Link Length

We now consider a more general case of one-dimensional linear network, the network with variable link length. Unlike the linear network with same link length
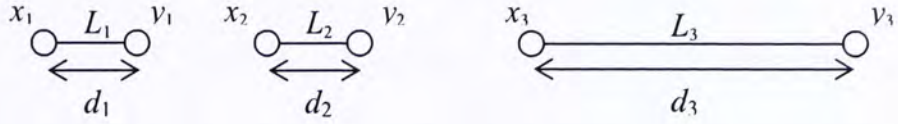
Figure 6-2: An example of linear network with variable link length

which has been discussed in Section 6.1.1, the conflict relationship of the links in a linear network with variable link length cannot be captured exactly by the intersection of intervals. An example of the linear network with variable link length is shown in Figure 6-2.

In Figure 6-2, suppose inequalities (13) to (15) are satisfied.

$$|x_2 - y_1| \geq (1+\Delta)d_1 \tag{13}$$

$$|x_2 - y_1| \geq (1+\Delta)d_2 \tag{14}$$

$$|x_3 - y_1| \leq (1+\Delta)d_3 \tag{15}$$

(13) and (14) mean links L_1 and L_2 do not interfere with each other, so there is no edge drawn between vertices v_1 to v_2 in the corresponding conflict graph. (15) shows that the transmission in L_1 will interfere with L_3, so there is an edge drawn between v_1 and v_3. This edge formation becomes impossible in an interval graph. v_1 is on the left of v_2, while v_3 is on the right of v_2. Therefore, if the interval of v_1 overlaps with the interval of v_3, it must overlap with the interval of v_2. i.e. in the interval graph, if an edge is drawn from v_1 to v_3, there must be an edge drawn from v_1 to v_2.

In the following paragraphs, we present our analysis of the one-dimensional linear network.

Definition 3: One-Dimensional Linear Network

It is a network in which nodes are positioned on the real line. The node in the left position of Link, L_i, is denoted by x_i, while the node in the right position of L_i is denoted by y_i. We assume the link length $d_i = y_i - x_i > 0$. In the corresponding conflict graph, each link L_i corresponds to a vertex v_i.

Definition 4: Vertex Labeling

We label the vertices (links) according to the left positions of the links. Specifically, if $x_i < x_j$ then $i < j$; and if $x_i = x_j$ then either $i > j$ or $i < j$. After such labeling, we can then draw the conflict graph associated with the linear network such that v_i is on the left of v_j if $i < j$.

It is worth reiterating that in this section we consider a general wireless network, not specific to any standard protocols such as 802.11. Therefore, carrier sensing mechanism is not taken into account. We give the following definition for edge formation in the conflict graph in a one-dimensional linear network.

Definition 5: Edge Formation

Consider two vertices, v_i and v_j, with $i < j$. There is an edge between v_i and v_j if and only if (16) is satisfied.

$$y_i + (1+\Delta)\max[d_i, d_j] > x_j \tag{16}$$

The corresponding conflict graph of the network in Figure 6-2 is shown in Figure 6-3. As explained by (13) to (15), edges are drawn between v_1 and v_3, and between v_2 and v_3. But no edge is drawn between v_1 and v_2.

Lemma 1: Consider two vertices v_i and v_j, with $j > i+1$. If there is an edge between v_i and v_j, then there is an edge between v_k and v_i , or an edge between v_k and v_j, for any k between i and j (i.e., $i < k < j$)

Proof: By definition 5, an edge between v_i and v_j means

$$y_i + (1+\Delta)\max[d_i, d_j] > x_j.$$

Case 1: $y_k \leq y_i$

In this case,

$$y_i + (1+\Delta)\max[d_i, d_k] > y_k > x_k.$$

By definition 5, there is an edge between v_k and v_i.

Case 2: $y_k > y_i$

Case 2.1: $y_k > y_i$ and $d_i \leq d_j$

In this case,

Figure 6-3: The conflict graph of the linear network in Figure 6-2

$$y_k + (1+\Delta)\max[d_k, d_j] > y_i + (1+\Delta)d_j = y_i + (1+\Delta)\max[d_i, d_j] > x_j$$

By definition 5, there is an edge between v_k and v_j.

Case 2.2: $y_k > y_i$ and $d_i > d_j$

$$y_i + (1+\Delta)\max[d_i, d_k] \geq y_i + (1+\Delta)d_i = y_i + (1+\Delta)\max[d_i, d_j] > x_j \geq x_k$$

By definition 5, there is an edge between v_k and v_i.

Corollary 2: *The conflict graph of a one-dimensional linear network cannot have a cycle of length $n \geq 5$ as its induced subgraph.*

Proof: We will prove the corollary by contradiction. Suppose that such a cycle exists as an induced subgraph. We re-label the vertices in the cycle while preserving definition 4, so that the vertices of the cycle are $v_1, v_2, v_3, ..., v_n$.

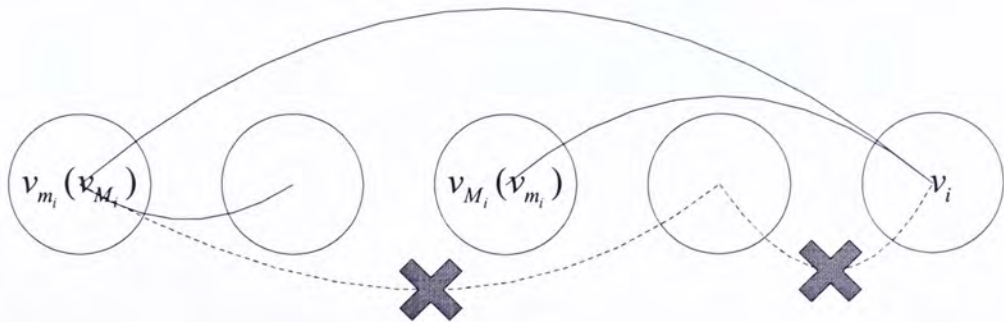*Observation 1:* A vertex v_i belonging to the cycle has two and only two edges.

Figure 6-4: Observation 2, $|i-m_i|$ should be less or equal to 3, otherwise, observation 1 is violated

Observation 2: Define v_{m_i} and v_{M_i} to be the two vertices in the cycle between which v_i has an edge. There are no more than two other vertices in the cycle between v_i and v_{m_i} (v_{M_i}). That is, $|i - m_i| \leq 3$ and $|i - M_i| \leq 3$. To see this, suppose that there are three vertices between v_i and v_{m_i} (v_{M_i}). Then, by Lemma 1, two of these vertices must both have an edge to either v_i or v_{m_i} (v_{M_i}) (Pigeonhole principle [33]). But then this will violate observation 1 above, since together with the edge between v_i and v_{m_i} (v_{M_i}), there will be three edges. Figure 6-4 shows this observation.

Consider the left most vertex v_1. Without loss of generality, suppose that $M_1 > m_1$. By observation 2, $M_1 \leq 4$. So, we have $1 < m_1 < M \leq 4$. There are only three cases to consider: 1) $M_1 = 3$, $m_1 = 2$; 2) $M_1 = 4$, $m_1 = 2$; and 3) $M_1 = 4$, $m_1 = 3$.
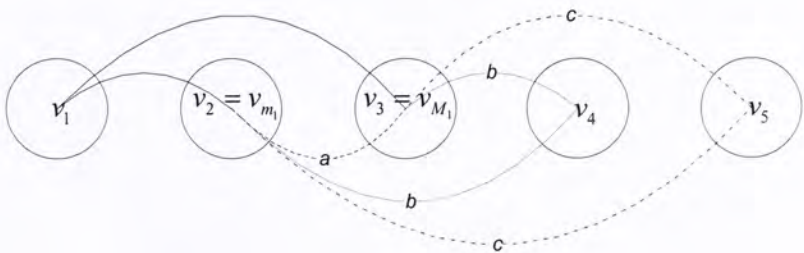

Figure 6-5: Case 1. If edge *a* is drawn, cycle of length 3 is formed. If edges of set *b* are drawn, cycle of length 4 is formed. If edges of set *c* are drawn, cycle of length 4 is formed. All edge drawings (*a*, *b* and *c*) lead to contradiction.

Case 1: $M_1 = 3$, $m_1 = 2$ (See Figure 6-5)

In this case, $v_{m_1} = v_2$ must have an edge with either v_3, v_4 or v_5 by observations 1 and 2. If v_2 forms an edge with v_3, we have identified a cycle of length 3 within the large cycle, leading to a contradiction. If v_2 forms an edge with $v_4(v_5)$, then by Lemma 1, v_3 has an edge with v_2 or $v_4(v_5)$, in which case we have identified a cycle of length 3 or a cycle of length 4, respectively, leading to a contradiction.

Case 2: $M_1 = 4$, $m_1 = 2$ (See Figure 6-6)

In this case, v_3 must have an edge with v_1 or v_4 by Lemma 1; however, it cannot have an edge with v_1 by observation 1. Now, v_2 must have an edge with v_3, v_4 or v_5. In the first case, a cycle of length 4 can be identified. In the second case, three edges will be found in v_4. As v_4 has already had edge with v_1 and v_3. This violates observation 1. In the last case, v_4 must have an edge with v_2 or v_5 by Lemma 1, causing v_4 to have three edges, violating observation 1.
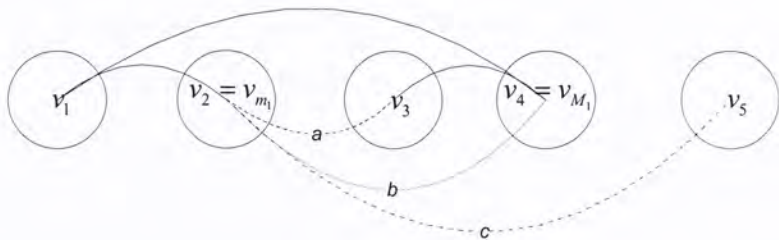
Case 3: $M_1 = 4$, $m_1 = 3$ (See Figure 6-7)

Figure 6-6: Case 2. If edge *a* is drawn, cycle of length 4 is formed. If edge *b* is drawn, three edges in v_4, violates observation 1. If edge *c* is drawn, v_4 must have one more edge to v_2 or v_5, violates observation 1. All edge drawings (*a*, *b* and *c*) lead to contradiction.
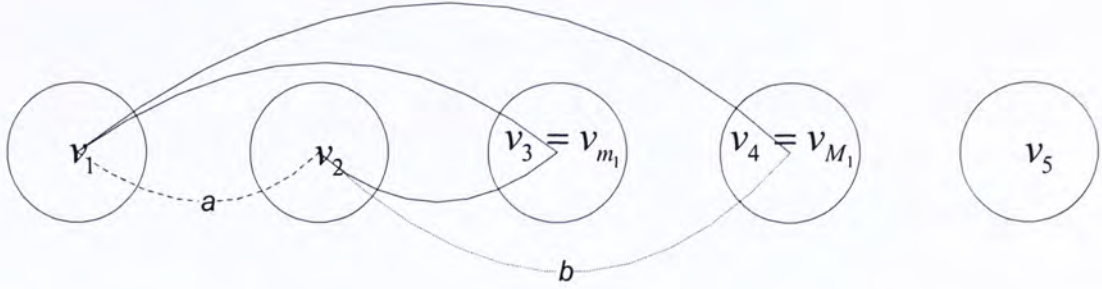
Figure 6-7: Case 3. By Lemma 1, v_2 must have an edge with v_3, as if edge a is drawn, there are three edges in v_1, violates observation 1. Similarly, by Lemma 1 and observation 1, edge b must be drawn. But drawing of edge b forms a cycle of length 4. It leads to contradiction.

Similar enumerative proof as cases 1 and 2.

Q.E.D.

Lemma 2: *Consider three vertices, v_i, v_k, v_j $(i < k < j)$ in the graph complement. If there is an edge between vertices v_i and v_k, and there is an edge between v_k and v_j, then there must be an edge between v_i and v_j.*

Proof: Lemma 1 about the original graph can be stated alternatively as "If there is no edge between v_i and v_k, and there no edge between v_k and v_j, then there must be no edge between v_i and v_j". This translates to Lemma 2.

Corollary 3: *The complement of the conflict graph cannot have a cycle of length $n \geq 5$, n odd, as its induced subgraph.*

Proof: We will prove the corollary by contradiction. Suppose that such a cycle exists as an induced subgraph. We re-label the vertices in the cycle while preserving definition 2, so that the vertices of the cycle are $v_1, v_2, v_3, ..., v_n$.

Observation 1:For odd n, there is a vertex v_k in the cycle such that there is an edge emanating from v_k to its left, say to vertex v_i; and another edge emanating from v_k to its right, say to vertex v_j. By Lemma 2 and observation 1, a cycle of length 3 is identified, leading to a contradiction.

To see observation 1, suppose that all vertices in the cycle either have both of their edges emanating to the left or to the right. We can rearrange the vertices into a bipartite graph so that the vertices with edges emanating to the left are positioned on the right column and the vertices with edges emanating to the right are on the left column. It can be easily seen that the number of left-column vertices must equal to the number of right-column vertices, which requires n to be even.

Q.E.D.

Corollaries 2 and 3 imply the conflict graph, G, of a one-dimensional linear network is perfect, i.e. $\chi(G) = \omega(G)$, by Strong Perfect Graph Theorem [34].

From the above result, we know that for a one-dimensional linear network, if we can keep the maximum clique size, $\omega(G)$, of its conflict graph, G, not exceeding the total available channels, the number of channels is in theory adequate for channel assignment to the linear network to isolate mutual interference. This provides a good reference for the call admission control in VoIP over wireless networks. For example,

in timeslot assignment of a linear network, we can admit the calls as long as the maximum clique size of its conflict graph not exceeding the total number of timeslots available.

6.2 Coloring of Two-Dimensional Network

The graph coloring problem becomes much more complicated when the network is a two-dimensional network. For simplicity, in this section we assume 802.11 network, and the two-dimensional network is under Hidden-node Free Design (HFD) [15]. As under HFD, the conflict graph of an 802.11 two-dimensional network can be modeled as a special class of graph, unit disk (UD) graph [35].

For HFD, all the nodes should set $CSRange \geq (3 + \Delta)d_{max}$, where d_{max} is the maximum link length [15]. So, the conflict graph of a two-dimensional network under HFD can be modeled as a UD graph, with the center of the disk (vertex of the graph) at the position of transmitter of a link, and the radius of the disk is $r = \dfrac{(3 + \Delta)d_{max}}{2}$. An edge is drawn between two vertices if their disks intersect with each other. In other words, it is a graph $G(V, d)$ has V as its set of vertices, and there is an edge between two vertices $v, w \in V$ if and only if $d(v, w) \leq d$, where $d(v, w)$ is the Euclidean distance between v and w. In our case, $d = 2r = CSRange$.

UD graphs are not necessary perfect. For example, we can simply construct a cycle of length 5 (see Figure 6-8), where its chromatic number is 3 while its maximum clique size is 2. Hence, for a UD graph G, $\chi(G) = \omega(G)$ does not always hold. It is also well-known that the UD graph coloring problem is NP-complete for each fixed number of colors $k \geq 3$. However, there are several approximations of the
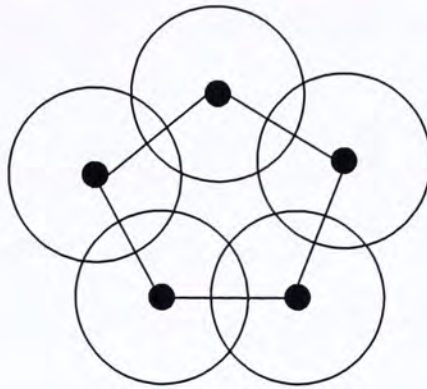
Figure 6-8: A cycle of length 5 formed in unit disk graph

chromatic number of UD graph, and approximating algorithms to color UD graph.

First of all, it is easy to find that the degrees in a UD graph G are always bounded from above by $6\omega(G)-7$, i.e. $\Delta(G) \leq 6\omega(G)-7$ [36]. So, $\chi(G) \leq 6\omega(G)-6$. A tighter bound, $\chi(G) \leq 3\omega(G)-2$, is also derived in [36] and [37] separately by different approaches.

In addition, [36] presents an algorithm, called STRIPE algorithm, which colors a UD graph G with at most $3\omega(G)$ colors. The main idea of the STRIPE algorithm is to partition the UD graph into a collection of subgraphs called stripes (with width $w \leq \dfrac{\sqrt{3}}{2} d$). By doing so, the subgraph can be proved to be a cocomparability graph (complement of comparability graph [38]) which is perfect. Each stripe can be colored optimally by Mohring's algorithm [39]. Then the coloring of G is obtained when the colored individual stripes are combined with the sequential permutative coloring (SPC) algorithm [36].

In timeslot assignment to VoIP over multiple WLANs, if the corresponding conflict graph is a UD graph (under HFD), we may apply the STRIPE algorithm and the

bounds above to find the allowable clique size in the network for call admission control. For example, if 802.11b is used and the UD graph is modeled, by applying the STRIPE algorithm, we find $3\omega(G) \leq 12$. It is because that 12 is the maximum number of timeslots available in VoIP over 802.11b WLAN. Then, the clique size should be controlled not larger than 4 by call admission control when we operate VoIP over multiple WLANs.

Obviously, the bound derived from the previous work is too conservative and it does not give practical impact in the engineering design of VoIP over multiple WLANs. In Section 4.3, we have found that even a heuristic algorithm is used, the maximum clique size could reach eight to ensure all admitted VoIP sessions meet the 1 to 3% packet-loss rate requirement. Therefore, a tighter bound for the maximum clique size in the conflict graph of VoIP over multiple WLANs to ensure the adequacy of the timeslots is needed, and it is an open research topic.

Chapter 7
Conclusion

VoIP over IEEE 802.11 WLAN is a research topic that has been attracting attention. In addition, commercial products (for example, Wi-Fi phone) have also been being developed. Much previous research work has studied VoIP over a single isolated WLAN. The IEEE 802.11e standard has also focused mainly on guaranteeing the QoS in a single isolated WLAN. In this thesis, we have demonstrated that the VoIP capacity can become extremely low when VoIP applications are deployed over multiple adjacent WLANs (i.e., the multi-cell scenario). In NS2 simulations, the per-AP capacity of VoIP over 5-by-5, 25-cell WLAN is only 1.63 sessions in 802.11b, and only 11.70 sessions in 802.11g.

The thesis sets up a conflict graph model for VoIP sessions over multiple WLANs. Based on the conflict graph model and the size of cliques formed in the graph, we have proposed a sophisticated clique-based call admission control algorithm. Compared with the simplistic call admission scheme, the clique-based call admission control algorithm can improve the per-AP VoIP capacity in a 5-by-5, 25-cell 802.11b WLAN by 52.1% to 2.48 sessions from 1.63 sessions. If three orthogonal frequency channels are applied, the call admission control can further boost the per-AP capacity to 7.39 VoIP sessions.

We have also investigated the integration of TDMA with the MAC of 802.11 networks to increase the VoIP capacity. Different from others' work, which mainly develops contention-free access to wireless medium through TDMA, we propose

coarse-grained TDMA (CTDMA). In each coarse timeslot, the stations access the wireless medium through contention-based algorithm, in particular CSMA in 802.11. We have found that with a small number (3 to 4) of coarse timeslots assigned, the per-AP VoIP capacity in multiple WLANs can be increased to 10 sessions in 802.11b or 58 sessions in 802.11g (another 35.3% improvement over clique-based admission control with three orthogonal frequency channels). In addition to the analytical and performance studies, we have also provided a preliminary feasibility study of CTDMA implementation within the 802.11 standard.

It is worth pointing out that the proposal of CTDMA not only has the benefits for VoIP applications over multiple WLANs, but also addresses the general problem of exposed nodes (EN) caused by inter-cell interference in IEEE 802.11 networks. In CTDMA, with the help of coarse timeslot assignment, carrier sensing range of nodes can be shortened to cover a smaller area, hence alleviating the EN problem and improving the overall system capacity.

We have used a graph theoretical approach to analyze the coloring in wireless networks. We have proved that the conflict graph of a one-dimensional linear network is a perfect graph. That means its chromatic number is equal to its maximum clique size. This implies that in theory, in channel assignment to VoIP over linear wireless networks, calls can be admitted until the maximum clique size is equal to the maximum available channels. Based on the previous work, we have also provided a preliminary discussion of the coloring problem in two-dimensional networks.

Further investigations to boost VoIP capacity over multiple WLANs could proceed

along the following directions.

1. **Reduction of header and protocol overheads** – Some previous research in single isolated WLAN has proposed related schemes. For example, packet aggregation methods [3], and burst transmission mode in IEEE 802.11e [21]. Further investigation is needed to apply such methods to 802.11 multi-cell scenario.

2. **Reduction of conflict edges** – Advanced 802.11-like protocols [19, 20], power control [40,41], or directional antennas [42] may help to isolate the mutual interference from neighboring cells in 802.11 networks. By reducing the edges in the conflict graph, more VoIP sessions can be added before the maximum capacity is reached.

3. **Call assignment schemes** – When a new call arrives, by some call assignment schemes, it will be assigned to an appropriate AP so that the overall capacity could be maximized. For example, sessions in hot-spot cells could be assigned and associated to adjacent cells [43].

4. **Exploration of frequency channel assignment methods** – Frequency channel assignment in 802.11 networks has been widely studied [47-50]. Based on some effective frequency channel assignments, such as "weighted coloring based channel assignment" [50] which assigns partially overlapping (non-orthogonal) frequency channels to WLANs according to the traffic loads, we could increase the performance of CTDMA.

Approach 1 is relevant to both single- and multi-cell scenarios while approaches 2, 3 and 4 are unique to the multi-cell scenario.

Appendices

Appendix 1

A MAC-Address-based Physical Carrier Sensing Scheme (MP)

A. How Carrier Sensing Affects EN

In traditional IEEE 802.11 carrier sensing, the MAC addresses of the sensed packet do not matter. Exposed node (EN) occurs when the carrier-sensing mechanism, which can be Physical Carrier Sensing (PCS) or Virtual Carrier Sensing (VCS) [11], disallows simultaneous transmissions by non-interfering links [45]. An example of EN is shown in Figure A-1. In this example, there are two wireless stations, N1 and N2, and two access points, AP1 and AP2. Links (N1, AP1) and (N2, AP2) are inside the *CSRange* but outside the *IR* of each other. So, simultaneous transmissions by the two links are not allowed, even though there is no mutual interference. We say that (N1, AP1) is exposed to (N2, AP2), and vice versa. EN is very common in the 802.11 basic-access mode as well as the RTS/CTS mode, and it is the fundamental factor
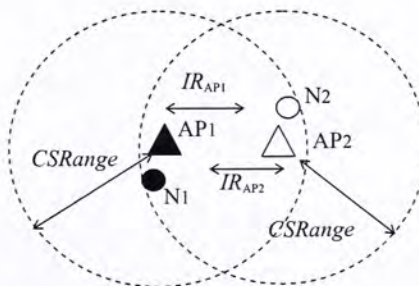

Figure A-1: An example of EN

limiting scalability of the Wi-Fi networks [44] due to inefficiency in spatial reuse.

MP can alleviate EN in large-scale WLANs. MP looks at the MAC addresses of the received packet and then selectively respects the PCS (not VCS as MP does not use RTS/CTS exchange) only if there is an interference relationship between the transmitting link and the link the node intends to transmit on. Consider the example in Figure A-1. Suppose that N1 is transmitting a packet to AP1, and N2 hears the packet from AP1 to N1. In MP, since the two links have no mutual interference (out of *IR* of each other), N2 will not respect the carrier sensing of the packet from N1 (does not treat the medium busy) and will go ahead to send a packet to AP2. Therefore, EN does not occur.

EN causes the formation of edges in the conflict graph of VoIP over multiple WLANs. By alleviating EN, the edges in the conflict graph can be reduced, and hence the VoIP capacity can be increased. So, MP can potentially increase the VoIP capacity over multiple WLANs.

B. Description of MP Protocol

MP implements a form of MAC-address-based Physical carrier sensing which depends on both the transmitter and receiver addresses of the packet being sensed, as well the transmitter and receiver addresses of the packet the node intends to transmit. The techniques needed to enable MP are described below.

For MAC-addressed-based PCS in MP, a node should be able to decode the MAC addresses once it decodes the PHY header. But in the conventional 802.11 (take IEEE 802.11b as an example) basic-access mode, the data rate of the PHY header is

1Mbps, with transmission range of 550m (which corresponds to the carrier-sensing range), while the data rate of the MAC header, which is encapsulated inside data payload (see Figure A-2), is 11Mbps, with transmission range of 250m. If the node is within the transmission range of the PHY header but outside the transmission range of the MAC header, the MAC addresses may not be decodable although the PHY header is decodable. Then, the node cannot perform PCS according to the MAC addresses. Therefore, for MP, the transmission range of PHY header and that of MAC addresses should be same. This means that the data rate of MAC addresses should be decreased to that of the PHY header. For simplicity, we propose to move the transmitter and receiver address fields to the PHY header so that they can be sent at 1Mbps as well (as shown in Figure A-3). Although the overhead of MP is larger than that of 802.11 Basic mode after moving the MAC addresses to the PHY header, MP can still have rather significant throughput performance improvements over the 802.11 Basic mode, as validated by simulation results presented in later paragraphs.

Figure A-4 shows a flowchart outlining the operation of MP. When the received signal power, P_{pkt} exceeds a receiver detection threshold P_{thresh}, the node will attempt
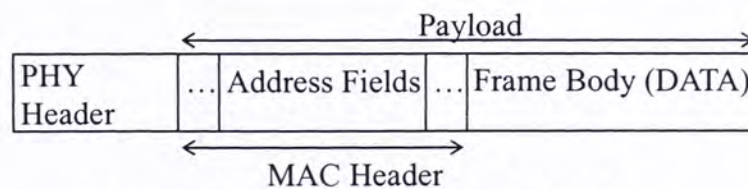

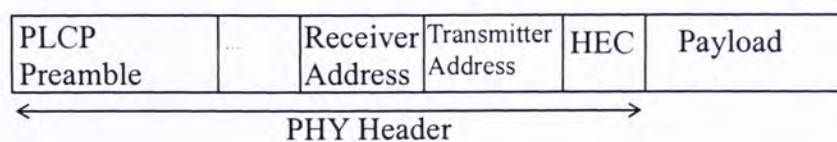**Figure A-2: Address fields in a DATA frame**

Figure A-3: PHY header of a DATA frame after adding MAC addresses

to receive the packet. The receiver detection threshold P_{thresh} here serves the same function as Clear-Channel-Assignment (CCA) threshold in the 802.11 standard [12]. The difference is that exceeding P_{thresh} here means there is possibly a "relevant" packet rather than a declaration that the channel is busy. The condition $P_{pkt} > P_{thresh}$ triggers the receiver to try to detect the packet, and to decide whether the channel is busy by following the steps as shown in Figure A-4 and as detailed below:
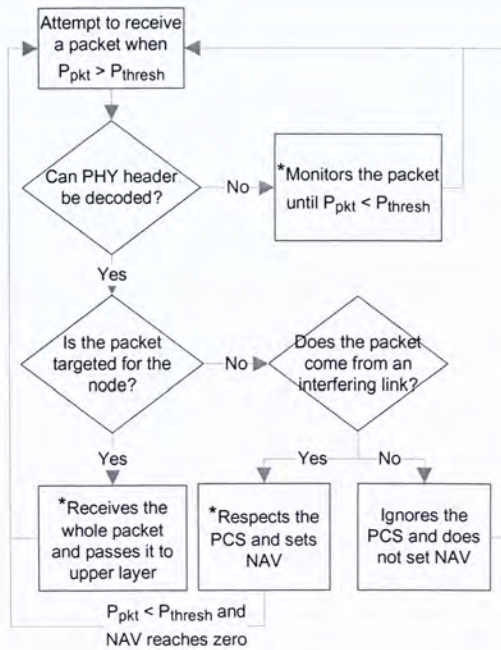

Figure A-4: The operation of MP protocol

(i) First, the receiver sees if the PHY header can be received correctly (using the HEC for parity check). If no, the node will treat the medium as busy and continue to monitor the packet until $P_{pkt} < P_{thresh}$. The fact that the PHY header cannot be received means there is perhaps a non-802.11 source (e.g., Microwave oven,

Bluetooth) transmitting at the same frequency band and they may cause collisions with the 802.11 transmissions. When $P_{pkt} < P_{thresh}$, following an EIFS (DIFS + ACK time), the node will go back to monitor the medium for another packet. In the state of continuous monitoring of the packet, the transmission mechanism and backoff counter are frozen until $P_{pkt} < P_{thresh}$. In Figure A-4, we include an asterisk for states in which the transmission and backoff mechanism is frozen.

(ii) If the PHY header can be decoded correctly, the node next decides whether the packet is destined for it. If yes, the whole packet is received and passed to the upper layer. While the packet is being received, the channel is also declared to be busy so that the transmission and backoff mechanism is frozen.

(iii) If the packet is targeted for other nodes, the node decides whether this packet is from a link that has an interfering relationship with the link the node intends to transmit on. (a) If there is interference relationship, then the normal PCS operation as in the conventional 802.11 basic mode will be conducted, including setting the NAV according to the packet length information extracted from the PHY header. (b) If there is no interference relationship, the node will treat the medium as idle and go back to monitor the medium for the next packet. Thus, there is no asterisk for case (b), and the transmission and backoff countdown mechanism can still be continued because the medium is treated as idle.

For normal CCA in the standard 802.11, (i) and (ii) are same. For (iii), normal CCA will always declare the channel to be busy without checking if the packet is from a link with an interfering relationship with the node. However, MP will divide (iii) further into cases (a) and (b). In (b), the channel will not be declared to be busy. In

addition, the receive detection threshold P_{thresh} will be increased by an amount corresponding to the power of the current signal being heard. When the current signal is no longer detected, P_{thresh} is decreased back to the original value.

C. Performance Evaluation of MP

Consider a square area of D by D, with M^2 equal-sized cells inside the area. Within the area, a total of $4M^2$ wireless client stations are randomly placed with a uniform distribution. An AP is located at the center of each cell. Each client station associates with the nearest AP. On average, four clients associate with each AP. We then generate a saturated UDP flow from each client to its associated AP. In the simulation, D is set to be 700m and M is set to be 5. We have carried out simulations for different UDP packet sizes: 50-byte, 210-byte, 500-byte and 1460-byte packets. We use 50-byte packets to simulate VoIP packets [3]. The topology used is the 5x5 grid. We fix the PCS range at 550m as the default value in NS2.
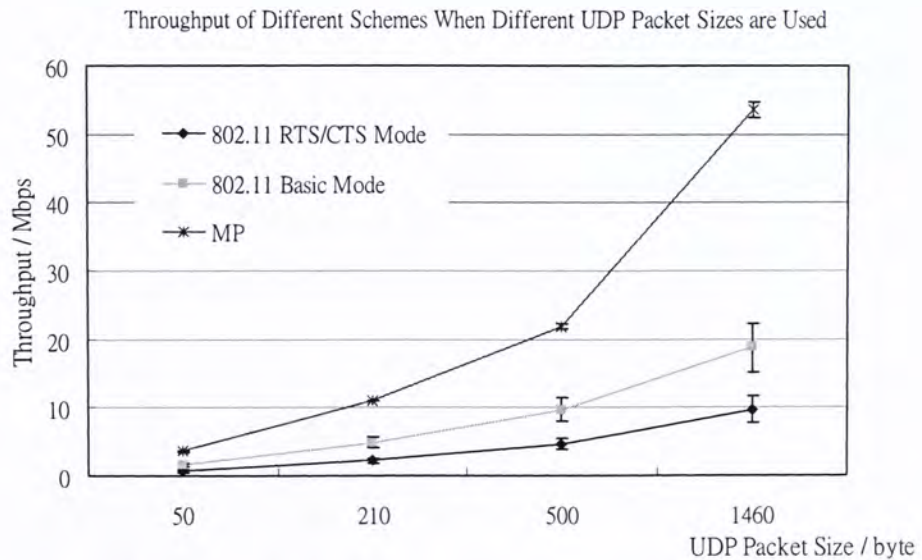
Throughput of Different Schemes When Different UDP Packet Sizes are Used

Figure A-5: Throughput of different schemes in 5-by-5 grid topology when different sizes of UDP packets are used

74

In Figure A-5, the total network throughput of different schemes is shown with 95% confidence interval. We find that MP outperforms standard 802.11 Basic and RTS/CTS modes. However, when small UDP packets are used, the throughput improvement by MP over 802.11 Basic Mode becomes smaller. It is due to its large packet header overhead.

D. MP Protocol and VoIP over WLAN

In this section, we analyze the packet header overhead of MP. The two important factors which affect the overhead of a transmission protocol is T_{trans}, the total airtime needed to complete a transmission, and T_{data}, the airtime used for transmitting the pure data content in DATA packet (i.e., $T_{packet} - T_{packet\_h}$, where T_{packet} is packet transmission time, and T_{packet_h} the transmission time for PHY, MAC headers and a CRC checksum which is appended to the packet). Refer to Figure 2-1, T_{trans} in MP and that in 802.11 Basic mode are given by (A1) and (A2) respectively.

$$T_{trans} = T_{backoff} + T_{DIFS} + T_{packet\_MP} + T_{SIFS} + T_{ACK} \qquad (A1)$$

$$T_{trans} = T_{backoff} + T_{DIFS} + T_{packet\_Basic} + T_{SIFS} + T_{ACK} \qquad (A2)$$

where $T_{backoff}$ is the countdown time of the backoff counter before transmission starts; T_{DIFS} is the time for Distributed Coordination Function (DCF) interframe space (DIFS) [11]; T_{SIFS} is the time for short interframe space (SIFS); T_{packet_X} is the time for transmitting a DATA packet in protocol X (which is MP or 802..11 Basic mode) (i.e. $T_{data} + T_{packet\_b}$); and T_{ACK} is the time for transmitting an ACK frame.

T_{trans} in MP and that in 802.11 Basic mode are same except their DATA packet transmission time. From Section C, we know that in MP, MAC address fields are

Table A-1: Sizes of Different Headers and Fields in a Typical IEEE 802.11 DATA Frame

Header / Field	Size (Byte)
PHY	24
MAC (Address Fields + Other Fields)	24 (18+6)
CRC	4

moved to the PHY header of the DATA packet and transmitted with the data rate as same as for other fields in PHY header. Take 802.11b as an example, PHY header is sent with 1Mbps, while the payload is sent with 11Mbps. According to Table A-1, (A3) and (A4) calculate $T_{packet\_h\_MP}$ (airtime used for transmitting packet header, which includes PHY, MAC headers and a CRC checksum, in MP) and $T_{packet\_h\_Basic}$ (airtime used for transmitting packet header in 802.11 Basic mode).

$$T_{packet\_h\_MP} = (24+18) \times 8 + (6+4) \times 8 / 11 \approx 343 \mu s \qquad (A3)$$

$$T_{packet\_h\_Basic} = 24 \times 8 + (18+6+4) \times 8 / 11 \approx 212 \mu s \qquad (A4)$$

In VoIP over WLAN application, T_{data} is very small, the typical value is around $24\mu s$ (i.e. payload is 33 bytes). From (A5), we find that the airtime used for transmitting packet header in MP is even larger than the airtime used for transmitting the whole data packet in 802.11 Basic mode.

$$T_{packet\_h\_MP} \approx 343 \mu s > T_{packet\_h\_Basic} + T_{data} = T_{packet\_Basic} \approx 236 \mu s \qquad (A5)$$

Therefore, MP is not suitable for applying on VoIP over WLANs although it significantly increases the total system throughput when data packet size is large. The slightly higher total throughput attained by MP than 802.11 Basic mode when UDP packet size is 50 bytes (shown in Figure A-5) is due to the so-call Receiver

Restart (RS) mode which is incorporated in MP protocol. In Appendix 2, we discuss the impact of applying the RS mode on VoIP capacity over multiple WLANs.

Appendix 2

Receiver Restart (RS) Mode

Here we consider another dimension to squeeze in more VoIP capacity: reducing the edges among the vertices in the conflict graph. Receiver Restart (RS) Mode [15] is incorporated into some commercial 802.11 chips (e.g. Atheros Chip). With RS, the receiver switches to receive a new signal in the midst of receiving an old signal if the new signal has a power stronger than the old signal by a certain threshold, say 10dB. This mode changes the interaction among links and may reduce the edges in the conflict graph.

To understand and model the effect of RS Mode, we need to consider the two
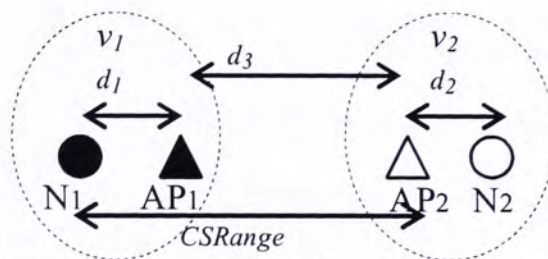
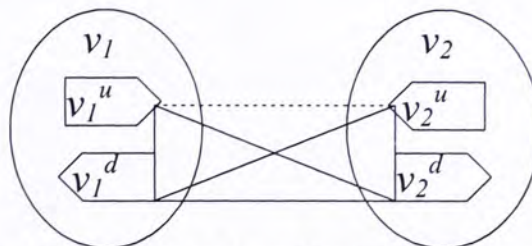**Figure A-6a: An example to show the effect of RS Mode**

Figure A-6b: The corresponding direction-aware conflict graph

transmission directions of a VoIP session separately. Let us split each vertex in the conflict graph into two vertices, v_i^u and v_i^d, representing the uplink (client station to AP) and downlink (AP to client) of v_i separately (as shown in Figure A-6a and A-6b). We shall refer to this conflict-graph model as "direction-aware conflict graph model", and the previous conflict-graph model as "direction-oblivious conflict graph model".

We illustrate the idea in Figure A-6a and A-6b. In the figures, we assume the distances between nodes to satisfy (A6) and (A7).

$$(1+\Delta)d_1 < d_3 \qquad \text{(A6)}$$

$$(1+\Delta)d_2 < d_3 \qquad \text{(A7)}$$

where Δ is the distance margin for interference-free reception. According to [15], once (A6) and (A7) are satisfied, the two VoIP sessions (v_1 *and* v_2) will not interfere with each other. But their carrier sensing mechanism may still affect each other because the *CSRange* in 802.11 is a fixed value that does not change with link distance. In Figure A-6a, the *CSRange* of N1 covers AP2, so an edge should be drawn between v_1 and v_2 in the direction-oblivious conflict graph. In the direction-aware graph (see Figure A-6b), this edge may be mapped to a maximum of six edges. First, there is always an edge between v_1^u and v_1^d, and an edge between v_2^u and v_2^d, respectively, by the assumption of half-duplexity. Then, there are the four potential edges between the pair v_1^u and v_1^d, and the pair v_2^u and v_2^d.

Consider the interaction between v_1^u and v_2^u. Suppose that N1 sends a packet to

AP₁ first, followed by N₂ sending a packet to AP₂ (note that N₂ can send a packet because it is not covered by the *CSRange* of N₁). If the RS Mode is not turned on, then AP₂ will not respond to the packet from N₂ even though the two VoIP sessions actually can transmit concurrently with no conflict according to the relationships in (A6) and (A7). The commercial 802.11 product commonly operates without RS by default although some chips (e.g. Atheros Chip) have incorporated RS as an optional mode. The default operation mode in NS2 is also without RS. Accordingly, there should be an edge between v_1^u and v_2^u without RS mode.

On the other hand, with RS, AP₂ will switch to receive the new signal from N₂ and respond with an ACK. That is, there is no edge between v_1^u and v_2^u with RS in the direction-aware conflict graph. Therefore, with RS, the number of edges is reduced and more VoIP sessions can be potentially admitted to the WLAN before C_{max} is reached. For the direction-aware conflict graph, C_{max} should be changed to a larger value (say 18) because of the bi-directionality (i.e., slightly more than two times the value of C_{max} in the direction-oblivious conflict graph model). Our simulation results show that RS mode can yield another 21% capacity improvement over clique-based call admission control in a 5-by-5, 25-cell WLAN, so that 3.00 VoIP sessions per AP can be supported.

References

[1] F. Anjum et al, "Voice performance in WLAN networks – an experimental study," *Proceedings of IEEE Globecom'03*, vol. 6, pp. 3504-3508, Dec. 2003.

[2] S. Garg, M. Kappes, "An experimental study of throughput for UDP and VoIP traffic in IEEE 802.11b networks," *Proceedings of IEEE WCNC'03*, vol. 3, pp. 1748-1753, Mar. 2003.

[3] W. Wang, S. C. Liew, Q. X. Pang, and V. O.K. Li, "A multiplex- multicast scheme that improves system capacity of Voice-over-IP on wireless LAN by 100%," *The Ninth IEEE Symposium on Computers and Communications*, June 2004.

[4] D. P. Hole, F. A. Tobagi, "Capacity of an IEEE 802.11b wireless LAN supporting VoIP," *Proceeding of the IEEE ICC'04*, vol. 1, pp. 196-201, Jun. 2004.

[5] W. Wang, S. C. Liew, V. O. K. Li, "Solutions to performance problems in VoIP over 802.11 wireless LAN," *IEEE Trans. on Vehicular Technology*, vol. 54, no. 1, Jan. 2005.

[6] "The Network Simulator – ns2," http://www.isi.edu/nsnam/ns/.

[7] P. Gupta, P. R. Kumar, "The Capacity of Wireless Network", *IEEE Trans. on Information Theory*, Vol. 46, No. 2, pp.388-404, Mar. 2000.

[8] Ashish Agarwal and P. R. Kumar, "Capacity bounds for ad-hoc and hybrid wireless networks." *ACM SIGCOMM Computer Communications Review, Special Issue on Science of Networking Design*, pp. 71-81, Vol. 34, No. 3, July 2004.

[9] G. Bianchi, "Performance analysis of the IEEE 802.11 distributed coordination function," *IEEE Journal on Selected Areas in Communications*, vol. 18, No. 3, Mar. 2000.

[10] A. Chan and S. C. Liew, "VoIP Capacity over Multiple WLANs", IEEE International Conference on Communications, Jun., 2007.

[11] M. S. Gast, "802.11 Wireless Networks: Definitive Guide," O'Reilly, Sebastopol, CA, 2002.

[12] IEEE Standard for Information Technology - Telecommunications and information exchange between systems - Local and Metropolitan networks - Specific requirements - Part 11: Wireless LAN Medium Access Control (MAC) and Physical Layer (PHY) specifications: Higher Speed Physical Layer (PHY) Extension in the 2.4 GHz band.

[13] Standard for Information Technology - Telecommunications and Information Exchange Between Systems - Local and Metropolitan Area Networks - Specific Requirements - Part 11: Wireless LAN Medium Access Control (MAC) and Physical Layer (PHY) Specifications: Further Higher Data Rate Extension in the 2.4 GHz Band, 2003.

[14] IEEE Standard for Telecommunications and Information Exchange Between Systems - LAN/MAN Specific Requirements - Part 11: Wireless Medium Access Control (MAC) and physical layer (PHY) specifications: High Speed Physical Layer in the 5 GHz band.

[15] L. Jiang, S. C. Liew, "Removing hidden nodes in IEEE 802.11 wireless networks," *IEEE Vehicular Technology Conference*, Sep. 2005. More comprehensive version to appear as "Hidden-node removal and its application in cellular WiFi networks," *IEEE Trans. On Vehicular Technology*, Nov 2007.

[16] "Clique (graph theory)," http://en.wikipedia.org/wiki/Clique_%28graph_ theory%29.

[17] L. Cai, X. Shen, J. W. Mark, L. Cai, Y. Xian, "Voice capacity analysis of WLAN with imbalanced traffic," Proceedings of *Qshine'05*, Aug. 2005

[18] "Maximal Clique", http://en.wikipedia.org/wiki/Maximal_clique.

[19] P. C. Ng, S. C. Liew, L. Jiang, "Achieving scalable performance in large-scale IEEE 802.11 wireless networks," Proc. of IEEE WCNC'05, Mar. 2005.

[20] A. Chan and S. C. Liew, "Merit of PHY-MAC cross-layer carrier sensing: a MAC-address-based Physical Carrier Sensing scheme for solving hidden-node and exposed-node problems in large-scale Wi-Fi networks," *The 6th IEEE Workshop on Wireless Local Networks*, Nov 2006.

[21] IEEE Std. 802.11e, "Part 11: Wireless LAN Medium Access Control (MAC) and Physical Layer (PHY) specifications. Amendment 8: Medium Access Control (MAC) Quality of Service Enhancements," Nov. 2005.

[22] J. Snow, W. Feng and W. Feng, "Implementing a low power TDMA protocol over 802.11," Proc. of IEEE WCNC'05, vol. 1, pp. 75-80, Mar. 2005.

[23] S. Sharma, K. Gopalan, N. Zhu, G. Peng, P. De, and T.-C. Chiueh., "Implementation experiences of bandwidth guarantee on a wireless LAN," Proc. ACM/SPIE Multimedia Computing and Networking, Jan. 2002.

[24] T. Chiueh and C. Venkatramani, "Design, implementation, and evaluation of a software-based real-time Ethernet protocol," ACM SIGCOMM Computer Communication Review, vol. 25, no. 4, pp. 27-37, 1995.

[25] K. M. Sivalingam, J. C. Chen, P. Agrawal and M. B. Srivastava, "Design and analysis of low-power access protocols for wireless and mobile ATM networks," Wireless Networks, vol. 6 no. 1, pp. 73-87, Feb. 2000.

[26] F. N. Ali, et al., "Distributed and Adaptive TDMA Algorithms for Multiple-Hop Mobile Networks," IEEE MILCOM'02, pp. 546-551, Oct. 2002.

[27] A. Kanzaki, T. Hara, S. Nishio, "An Adaptive TDMA Slot Assignment Protocol in Ad Hoc Sensor Networks," ACM SAC'05, Santa Fe, USA, Mar. 2005.

[28] Z. Cai, M. Lu, "SNDR: a new medium access control for multi-channel ad hoc networks," IEEE VTC'00, Tokyo, Japan, May 2002.

[29] D. J. A. Welsh and M. B. Powell, "An upper bound for the chromatic number of a graph and its application to timetabling problems," The Computer Journal 10, pp.85-86, 1967.

[30] C. W. Sung and W. S. Wong, "Sequential Packing Algorithm for Channel Assignment Under Cochannel and Adjacent-Channel Interference Constraint," *IEEE Trans. on Vehicular Technology*, vol. 46, no. 3, Aug. 1997.

[31] "Interval graph," http://en.wikipedia.org/wiki/Interval_graph.

[32] "Perfect graph," http://en.wikipedia.org/wiki/Perfect_graph

[33] "Pigeonhole principle," http://en.wikipedia.org/wiki/Pigeonhole_principle

[34] "Strong Perfect Graph Theorem," http://mathworld.wolfram.com/StrongPerfectGraphTheorem.html

[35] "Unit disk graph," http://en.wikipedia.org/wiki/Unit_disk_graph

[36] A. Graf, M. Stumpf, and G. Weibenfels, "On coloring unit disk graphs," *Algorithmica*, 20(3):277-293, 1998.

[37] R. Peeters, "On coloring j-unit sphere graphs," *FEW 512*, Department of Economics, Tilburg University, NL, 1991.

[38] "Comparability graph," http://en.wikipedia.org/wiki/Comparability_graph

[39] R. H. Mohring, "Algorithmic aspects of comparability graphs and interval graphs," *Graphs and Orders*, pages 41-101. D. Reidel Publishing Company, 1985.

[40] W. H. Ho and S. C. Liew, "Achieving Scalable Capacity in Wireless Networks with Adaptive Power Control," *The 5th IEEE Workshop on Wireless Local Networks*, Nov 2005.

[41] W. H. Ho and S. C. Liew, "Distributed Power Control in IEEE 802.11 Wireless Networks," *IEEE International Conference on Mobile Ad-hoc and Sensor System (MASS)*, Oct 2006

[42] J. Zhang and S. C. Liew, "Capacity Improvement of Wireless Ad Hoc Networks with Directional Antennae," *IEEE Vehicular Technology Conference*, May 2006.

[43] S. C. Liew and Y. J. Zhang, "Proportional Fairness in Multi-channel Multi-rate Wireless Networks," *IEEE Globecom 2006*, Nov 2006.

[44] L. Jiang, "Improving Capacity and Fairness by Elimination of Exposed and Hidden Nodes in 802.11 Networks," *M.Phil Thesis*, The Chinese University of Hong Kong, Jun. 2005.

[45] S. Grag and M. Kappes, "Admission Control for VoIP Traffic in IEEE 802.11 Networks," IEEE Globecom 2003, Dec 2003.

[46] S. Ramanathan, "A Unified Framework and Algorithm for (T/F/C)DMA Channel Assignment in Wireless Networks," IEEE INFOCOM 1997, Apr 1997.

[47] J. Geier, "Assigning 802.11b Access Point Channels," Wi-Fi Planet.

[48] Y. Lee, K. Kim and Y. Choi, "Optimization of AP Placement and Channel Assignment in Wireless LANs," LCN 2002, Nov 2002.

[49] K. Leung and B. Kim, "Frequency Assignment for IEEE 802.11 Wireless Networks," VTC 2003, Oct 2003.

[50] A. Mishra, S. Banerjee and W. Arbaugh, "Weighted Coloring Based Channel Assignment for WLANs," ACM SIGMOBILE 2005, Jul 2005.